nillinen korkeakoulu
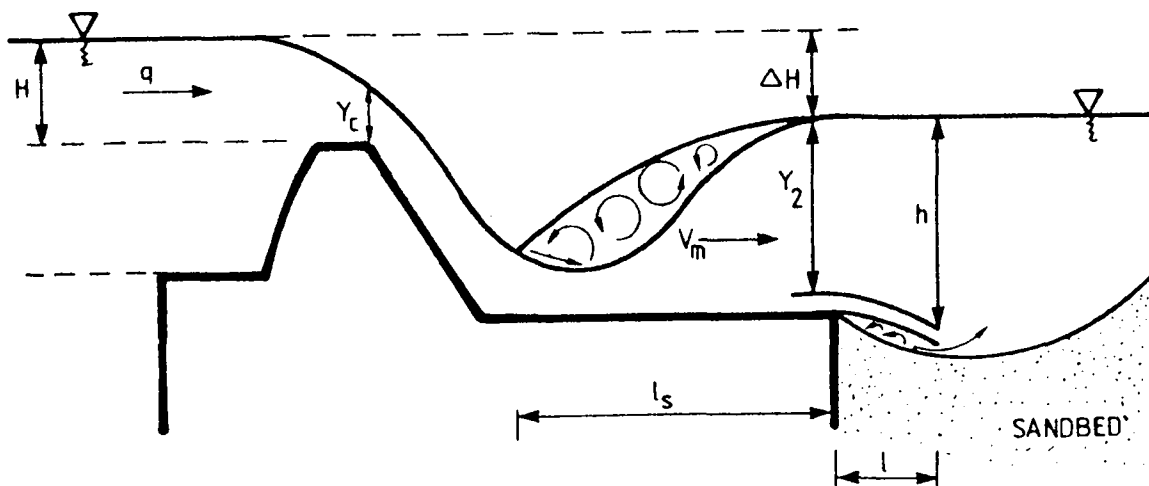
kan osasto

sity of Technology

Civil Engineering

Water Supply and Sanitation

Post Graduate Course in Water Engineering 1982-84

N:o B2

In co-operation with
Finnish International Development Agency
FINNIDA

Bayou Chane

Two-dimensional Local Scour in Erodible Bed Downstream of Solid Aprons

Tampere 1984

TWO-DIMENSIONAL LOCAL SCOUR IN ERODIBLE BED
DOWNSTREAM OF SOLID APRONS

by

BAYOU CHANE

Thesis submitted to the department
of civil engineering, Tampere
University of Technology, in
partial fulfillment of the
requirements for the degree of
Master of Science in Engineering.

February 1984
Tampere, Finland

To my parents
and
my fiancee

ACKNOWLEDGEMENTS

TWO-DIMENSIONAL LOCAL SCOUR IN ERODIBLE BED
DOWNSTREAM OF SOLID APRONS

TABLE OF CONTENTS   Page

ABSTRACT

This paper deals with two dimensional local scour in an erodible bed below solid apron resulting from residual energy of stream flow leaving the hydraulic jump basin.

A comprehensive discussion of the topic is given based on literature survey. Factors influencing local scour are mentioned. The stability of descrete particles under a stream flow is briefly explained. Different stages of the process of scour hole development and the effect of clear and sediment loaded water on the latter are presented and discussed. An assessment is made of scour hole profiles obtained from varying magnitudes of bed material type, stream flow,and apron length in order to observe the existence of similarity between them. The influence of bed material type, apron length, appurtenances of stilling basins, and of flow characteristics on the ultimate magnitudes of length and depth of scour hole are presented and discussed. Ways of predicting the depth of scour hole are pointed out. Similarity criteria required to reproduce the same type of flow in a scale model as in its prototype, the criteria of model scale selection, and time scale between model and prototype local scour are explained. Prevention of local scour by using energy dissipation devices and estimation of the region of erodible bed susceptible to local scour and the method of protection are also explained. Measuring techniques of the flow parameters related to local scour (bed topography, water level, flow velocities, discharge, and sediment transport), and measuring devices and instruments for the above are briefly presented.

GLOSSARY

clear-water scour
erosion worked out by the flow
of water which is free of sediment

depth of scour
the vertical measure from the
original bed level to the scour
hole profile

duration of scour
the time elapsed from the
beginning of erosion to the
final moment of investigation

erodible bed
the bottom of a channel consis-
ting of sand or gravel particles
which can be disloged by stream
flow when the critical shear
stress of the particles is over-
come by hydrodynamic shearing
force

excavation profile
end configuration of scouring
process in the alternating
processes of excavation and
filling

excavation stage
the part of scouring process,
in the alternating processes of
excavation and filling, in
which the erosion of the bed
takes place

filling profile
end configuration of the filling
process in the alternating
processes of excavation and
filling

filling stage — the part of scouring process, in the alternating processes of excavation and filling, in which the filling of the scour hole takes place

length of scour downstream end of solid — the horizontal measure from the downstream end of solid apron to the section where the scour hole profile reattaches itself with the original bed level

local scour — the process of concentrated erosion and degradation

maximum scour depth — the measure of the deepest section in a scour profile

pot hole scouring — the stage of scouring following the sheet scouring characterized by separation of flow

sheet scouring — the earliest stage of scouring in which the whole of the upper layer of particles in the erodible bed appear to be in movement in the general direction of flow

solid apron — the paved floor of a stilling basin constructed to protect the scouring of the erodible bed laying under it

sounding — the method of measuring the depth of bed topography by means of a weighted line controlled from a boat or cableway

time scale   the rates of duration of local scour in a prototype structure to the duration of local scour in its model

ultimate depth of scour   the scour depth corresponding to the state of equilibrium of the local scour process

zone of flow tranzition   also term as tranzition zone; the region from the end of the hydraulic jump to a downstream section at which the high turbulence intensity due to the change of flow characteristics at the jump is diminished and the normal channel flow characteristics are restored

1. INTRODUCTION

When a dam, barrage, spillway, or a weir is built across a
river or canal, it becomes an obstruction to the natural regime
of the system. Such an obstruction modifies the flow
characteristics in the neighbourhood (upstream and down-
stream) of its location. Upstream from the obstruction,
the flow is slowed down as far as the upstream edge of the
reservoir or impoundment is reached, at which it maintains
the natural regime. On this side of the obstruction, the
process of sedimentation and aggradation takes place. What
is happening upstream of the obstruction is not the main
concern of this paper.

A net head of water exists due to the elevation difference
between the head water level and tailwater level. Potential
energy proportional to the available net head is stored in
the impounded water. When the water flows across the
obstruction, the potential energy is changed into kinetic
energy. This results in a high velocity of flow at the toe
of the structure.

Most commonly, a large quantity of the kinetic energy is
dissipated by creating a hydraulic jump on a solid apron
of economical length. However, a significant amount of the
energy which is estimated to be about 30 to 50 % of the
energy before dissipation still, remains in the flow after
the hydraulic jump /20/.

The velocity of the flow due to the residual energy after
the hydraulic jump is comparatively higher than the velocity
in the normal channel flow which could have occured had
there not been any obstruction across the channel. This
high velocity is one of the factors responsible for erosion
of moveable bed material.

A very high turbulence is created in the hydraulic jump.
The turbulence continues downstream and it modifies the
sediment transport capacity of the flow from the erodible
bed.

The system that has been in equilibrium prior to the
existence of the obstruction is distrubed, i.e., the
sediment supply rate and the transport capacity do not
much. The water which has lost almost all of its sediment
load on the upstream side has a very high potential to
carry a new sediment load.

Therefore, residual kinetic energy leaving the stilling
basin, the turbulence generated by the hydraulic jump, and
the high potential of the flow to carry new sediment load
work on the erodible bed immediately below the solid apron,
thereby, progressively degrading it and forming a hole.
This process of concentrated erosion and degradation is
called local sour, and the hole created as the result of
this process is called scour hole.

When dissipating energy by using hydraulic jump, it is
required that the jump occurs on a solid apron. However,
depending on the magnitude of discharge and the tailwater
condition, the jump may be out of control and may occur
partially on the erodible bed; or jump may not form at all.
The erosion taking place under such a condition of flow is
more severe than the erosion occuring when the jump is
controlled to form on the solid apron. Obviously, the worst
situation is when the high velocity flow over a spillway
or under a gate strikes directly on the erodible bed.

The scope of this paper is limited to local scour, due to
the residual energy, occuring downstream of the solid
apron in an erodible bed of non-cohesive material such as
sand and gravel.

A large size local scour can endanger the stability of a
solid apron below a weir by undermining the foundation
which is normally placed horizontally on the upper layers
of the river bed. This can cause a partial or complete
destruction of the hydraulic structure which may be
followed, in the worst case, by a great loss of life and
property other than the structure itself. Local scour is
the main cause for the complete destruction of the historical
dams in old Egypt /4/. They were well constructed structures
in comparison with the other living monuments of the past.
The major failure of the Islam weir in India (1929) is due
to local scour /24/. In recent times some modern small dams
were put out of operation because of localized scour.
Internationally known are the local scours produced in the
spillway of the Ricobayo dam /16/.

Therefore, local scour is among the most important hydraulic
problems which should deserve enough attention. It is
essential to study the problem and to be able to explain
its features so that the effects can be predicted. Predic-
tion of the ultimate dimensions of scour hole (profile,
depth, and length) expected downstream of a solid apron is
necessary. It helps to decide about the preventive and
protective measures of local scour problem. Economical and
safe structures can be selected and designed if and only
if the problem is well understood and explained. Lack of
this knowledge results in, either, expensive prevention
and protection structures, or, inadequate and unsafe ones.

2.   GENERAL

2.1 Local Scour Investigations in the Past

2.1.1 Actual Structures

Although it is known that the construction of dams and other
hydraulic structures is an old practice, it has remained
for many years very difficult to obtain adequate data and
reliable design principles to produce economical structures
which will remain safe during the expected service period.
Of the many hydraulic structures (dams, spillway, weirs,
barrages) which were damaged by different forces, some were
due to local scour downstream of the solid apron. Two
cases of observations made in actual structures are given
below.

The Islam barrage which is 494 m (= 1621 ft) in length is
divided into 24 openings each spaning 18.30 m (= 60 ft).
It has a downstream solid apron sloping down some distance
and then extending horizontally ending abruptly without
a cutoff wall. Downstream from the solid apron are placed
concrete blocks and heavy riprap. The barrage was put into
service in the spring of 1927. Due to high velocity flow
during floods, the erodible channel bed below the solid
apron decreased in level by 0.70 m (=2.3 ft), 1.70 m (=5.5 ft),
and 2.00 m (= 6.5 ft) in Nov/1927, Dec/1928, and May/1929,
respectively. The scour resulting from this drop was so
severe that a large portion of the downstream solid apron
was destroyed and finally six bays of the structure collapsed.
According to the opinion of Joglekar and Wadekar, this
failure due to scour of a major work may perhaps be the
most costly one./24/

Another case of scour development investigated in practice
is downstream of the Ganga weir at Hardawar.   The weir
is constructed across a boulder stage river. Progressive
scour of the talous downstream of the solid sloping apron

(20:1) became perceptible since the year 1933. The deepest
scour observed was 6.20 m (= 20 ft) in 1947. It was
observed that even at low flow stages, hydraulic jump did
not form at the toe of the glacis and the turbulent flow
beyond the solid apron caused the damage to the talous and
undesirable scour developed in the river bed downstream./18/

Many similar problems due to local scour have undoubtedly
occured below hydraulic structures of various functions
built across channels of erodible bottom. However, quanti-
tative data on the process of development and the ultimate
dimensions of local scour from actual structures is scanty
and inadequate. This could be one of the reasons which
has retarded the expansion of knowledge in local scour
problem.

Some of the reasons for scarcity of data are:

1. It is very difficult to measure the characteristics
    of the geometry of the scour hole in actual situation.

2. It is impossible to observe visually how the local
    scour development process takes place.

3. It is an expensive affair to allow damages of actual
    structures for the sake of investigation of scour,
    despite the fact that it helps to reduce future
    construction and maintenance costs.

4. It may take many years for the severe flow condition
    to occur, sometimes 20 to 30 years, and it is also
    somewhat difficult to know the actual time of occurence
    to be ready for measurement and investigation.

Nevertheless, the need for actual data is felt very much by
investigators of local scour phenomena for confirming the
experimental and scale model test results they obtain
under various conditions and limitations.

2.1.2 Experimental and Scale Models

Many engineering problems are solved through research by employing experimental and/or scale model studies. Devoted investigators have, likewise, carried out model studies in local scour problem with the intent of understanding and explaining the problem.

Literature survey on local scour development studies and related works reveals that the number of experimental model studies is much greater than the simulated model (scale model) studies and analytical approaches. In some of the studies, investigators have considered local scour development in general while in many others they have tried to emphasize the effect of particular parameters on the different features of local scour. General treatment of the problem can be found in the reports of Blench /6/ and Tsuchiya /44/.

The most important particular parameters which are considered by many investigators are: geometry of hydraulic works /2/ /53/17/13/9/30/; discharge per unit width /2/50/13/41/; quality of water /11/13/47/; type of flow /2/20/28/17/13/ /38/; Froude number /13/; type and particle size of bed material /2/17/50/30/, and evolution of scour hole /8/13/ /5/14/. In all the above mentioned studies local scour is treated as a two-dimensional problem. The two-dimensional treatment is prefered for simplicity of investigation and explanation. A few investigators, however, have studied it as a three-dimensional problem /49/13/48/.

In carrying out various studies of local scour problem, the main goal anticipated is to establish a rational approach which can enable us to predict practically acceptable scour dimensions in actual structures from laboratory scale model test results. In view of this, while many investigators are looking for relationships among the different parameters involved in the development of local scour, others are trying to establish similarity relations between subsequent

scour shapes /15/34/3/4/38./. The anticipated goal can be achieved if and only if similarity relations that will hold true between any size of scale models can be established. The problem will remain unsolved if similarity relations are restricted only to the laboratory scale models. A great effort must be made to obtain the criteria for similarity between the laboratory size scale models and prototype local scour dimensions.

2.2 Classification of Local Scour

According to the quality of the water flowing into the scour region, local scour is classified as clear-water scour and scour with sediment loaded water.

a) Clear-water scour:

As the name implies clear-water scour is the scour worked out by the flow of water which is practically sediment free. This occurs downstream of very common hydraulic structures like spillways and weirs.It is a more severe scour problem which has attracted the attention of most investigators. Clear-water scour formation and its progress is presented in sec. 3.2.1.

b) Scour with sediment loaded water:

The local scour which takes place with sediment carrying water flowing into the erodible region is refered to as scour with sediment loaded water. Sediment loaded water can reach the erodible bed during flows passing through bottom outlets or during high flood passing over spillways and weirs. The degree of scour for similar conditions of flow is less in scour with sediment transport than in clear-water scour (sec. 3.2.2).

2.3 Factors Affecting Local Scour

The following factors influence local scour in an erodible
bed below a solid apron:

1. Type of flow (flow pattern)
2. Discharge passing a unit width
3. Effective head (velocity)
4. Form of the stilling basin and energy dissipation
5. Apron length
6. Tailwater depth
7. Depth/velocity relation
8. The quantity of sediment material carried by the flow
9. Type of the erodible material constituting the bed
    (size, specific gravity, shape)
10. Flow duration over the erodible bed.

2.4 Stability of Discrete Particles under Stream

From the viewpoint of scouring of discrete particles under
the dynamic action of fluid flowing past them, there are
two classes of interacting forces:

1. destabilizing forces
2. stabilizing forces.

The destabilizing forces are the drag and lift forces and
the stabilizing one is the submerged weight of the particle.

The drag force is the result of surface drag (due to
viscous skin friction) and the form drag due to pressure
differences in front and behind the particle /35/. This
force is expressed as

$$F_D = C_D A \frac{\rho U^2}{2} \qquad (2.1)$$

or, it may be also expressed by

$$F_D = C_D K_1 D^2 \frac{\rho U^2}{2} \qquad (2.2)$$

where

C_D = drag coefficient,

ρ = density of fluid,

A = the characteristic projected area of the particle normal to the direction of flow,

U = the characteristic fluid velocity in the neighborhood of the particle,

K_1 = dimensionless particle shape-factor (projected area),

D = typical grain diameter of the surface particle.

A solid particle resting on the bottom of a channel is subjected to:

1. the turbulent velocity and velocity fluctuations and
2. a fluctuating hydrostatic pressure that varies in magnitude over the surface of the particle.

These variables determine the magnitude of the lift force. The vertical component of the turbulent flow added to the lift resulting from the inequality of the hydrostatic pressure acting on the particle gives the total lift force /42/. This force can be expressed as

$$F_L = C_L A \frac{\rho U^2}{2} \qquad (2.3)$$

or, it may be expressed as

$$F_L = C_L K_1 D^2 \frac{\rho U^2}{2} \qquad (2.4)$$

where

C_L = lift coefficient

A, ρ, U, K_1, and D are as in eqs. 2.1 and 2.2.

Usually, the lift force does not appear explicitly in theoretical analysis, because lift depends on the same parameters as drag and the constants in the resulting theoretical equation are determined empirically. This procedure automatically considers the effect of lift /42/. Therefore, the disturbing force on a typical particle is

$$F_{D,L} = (C_{D,L}) K_1 \cdot D^2 \frac{\rho U^2}{2} \qquad (2.5)$$

The submereged weight of the particle is given by

$$F_g = (\rho_s - \rho) g V_s \qquad (2.6)$$

or, it may also be given by

$$F_g = (\rho_s - \rho) K_2 D^3 \qquad (2.7)$$

where,

ρ_s = density of particle,

V_s = volume of particle,

g = acceleration due to gravity,

K_2 = dimensionless particle shape-factor (volume).

The sediment transport starts when the shear stress τ_s, created by the drag force of the flowing water overcomes the critical shear stress τ_c, i.e., when $\tau_s \geq \tau_c$. The expression for shear stress is

$$\tau_S = \rho U_*^2 \qquad (2.8)$$

where

ρ = density of water,

U_* = shear velocity,

and the expression for critical shear stress is

$$\tau_c = f_s (\gamma_s - \gamma) d \qquad (2.9)$$

where

f_s	=	constant factor,
γ_s	=	unit weight of sediment,
γ	=	unit weight of water,
d	=	diameter of sediment particles.

Einstein departed from the tractive force concept for sediment transport. According to him, in the turbulent flow the fluid forces acting on the particle vary with respect to both time and space, and therefore the movement of any particle depends upon the probability, p, that at a particular time and place the applied forces exceed the resisting forces. The definitions of the Einstein grain mobility parameter, ψ, and bed load parameter, ϕ, are

$$\psi = (\rho_s - \rho)\frac{gD}{\tau} \qquad\qquad (2.10a)$$

or $\qquad \psi = (S_s - 1)gDV_*^{-2} \qquad\qquad (2.10b)$

where,

ρ_s	=	density of particles,
ρ	=	fluid density,
g	=	gravitational constant ,
D	=	representative diameter of particles,
T	=	shear stress on the particles,
S_s	=	specific gravity of the particles,
V_*	=	shear velocity,

and $\qquad \phi = q_B(S_s-1)^{-1/2}(gD^3)^{-1/2} \qquad\qquad (2.11)$

where $\qquad F = \sqrt{\dfrac{2}{3} + \dfrac{36\gamma^2}{gD^3(S_s-1)}} - \sqrt{\dfrac{36\gamma^2}{gD^3(S_s-1)}} \qquad (2.12)$

q_B	=	volume rate of bed load discharge per unit width,
γ	=	kinematic viscosity.

The relationship between the bed load parameter and the
grain mobility parameter is expressed as

$$\phi = f(\psi) \tag{2.13}$$

3. SCOUR HOLE DEVELOPMENT

3.1 Stages of Scour Hole Development

3.1.1 Initial Stage

In the transition zone of the flow after the hydraulic jump,
the velocity distribution at a cross-section is such that
it is high close to the bed and decreases upwards which is
the reverse of the situation in open channel flows without
obstruction /44/28/. Of course, before a scour hole is
formed the surface particles of the erodible bed are exposed
to this high velocity. During the earliest stage of scouring,
the whole of the upper layer of particles in the erodible
bed appear to be in movement in the general direction of
the flow. This type of erosion is termed as sheet scouring
/50/. Typical scour profiles observed in a gravel bed are
shown in figure 3-1. Sheet scouring occurs prior to the
formation of profile A.
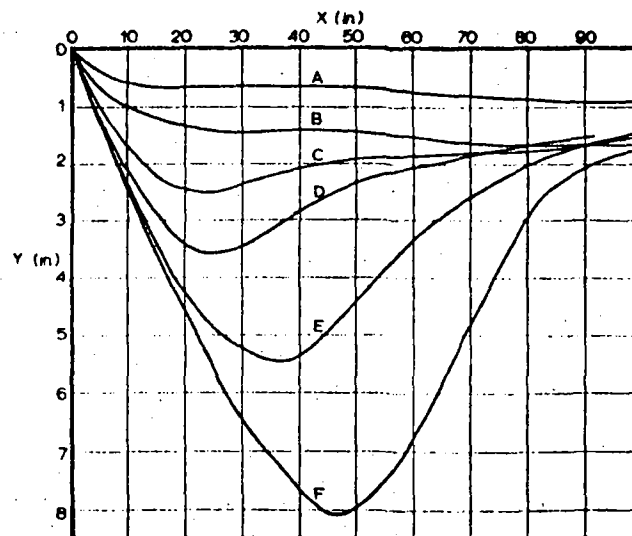
Figure 3-1. Typical scour profile; from tests on gravel.
(s= 0.83 ft/sec); V= 3.1 ft/sec./50/
A = scour profile at which sheet scouring ends
B = transition scour profile from sheet scouring
       to pot hole scouring
C,D,E,F= scour profiles resulting from pot hole scouring.

3.1.2 Progressive Stage

3.1.2.1 Region of Flow Separation

When the scour hole profile becomes deep enough as with
profile C in fig. 3-1, a separation region between the main
stream and the lower boundary, commencing at the edge of
the solid apron is distinguished. For convinience of
description this type of scouring (which produces bed forms
illustrated by the profile C onwards in fig. 3-1) is termed
as pot hole scouring / 50/. The point where the jet meets
the bed profile shifts its position with time. This point is
the deepest point of the scour hole. The flow splits into
two directions, one along the flow and the other against it,
as demonstrated by a schematic representation shown in
fig. 3-2 /2/50/.
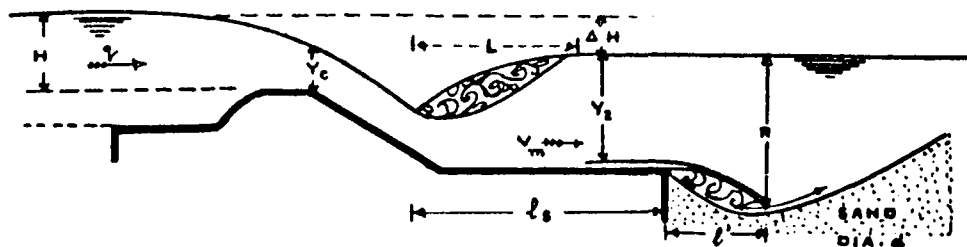
Figure 3-2.   Flow below a hydraulic work.

The reverse flow is made up of a roller which occupies the
flow separation region. This roller is given different names
by different investigators. Rehbock calls it ground roller
to distinguish it from surface roller of a standing wave,
and Butcher prefers to call it positive roller because of
its action in rolling the bed material up towards the solid
apron. /2/

3.1.2.2 Location of Peak Scour

Watkins has observed that in the lee of the roller, there
occured irregular patterns of eddies and jets of water which
were being detached from the main stream and the roller and
rejoined to the main stream before its reattachment to the
bed; thereafter the water movement was again mainly parallel
to the bed with superposed turbulent eddies. The most
vigorous scouring was in the bed adjacent to the region of
confused flow just downstream from the roller./50/

By considering relative turbulence intensity as the main
factor of local scour, Schoppmann, has reported that the
intensive shear zone, which is created by the separation of
flow, changes also the relative turbulence intensity near the
bed (it is three times higher than the value in the
undisturbed flow). A peak value of relative turbulence
intensity occurs, in some of the tests, near the point of
reattachement of flow, the relative location of which varied
in each scour hole, fig. 3-3. In his report Schoppmann has
stated that the peak value of the relative turbulence
intensity confirms the presence of large eddies created in
the shear zone and is mainly responsible for the sediment
transport out of the scour hole./ 41/

Ahmad has observed that the greatest and strongest eddies
are formed in the region of greatest discontinuity. These
eddies lift up the bed materials as long as the velocities
caused by them become equal to the fall velocity of the
particles. /2/
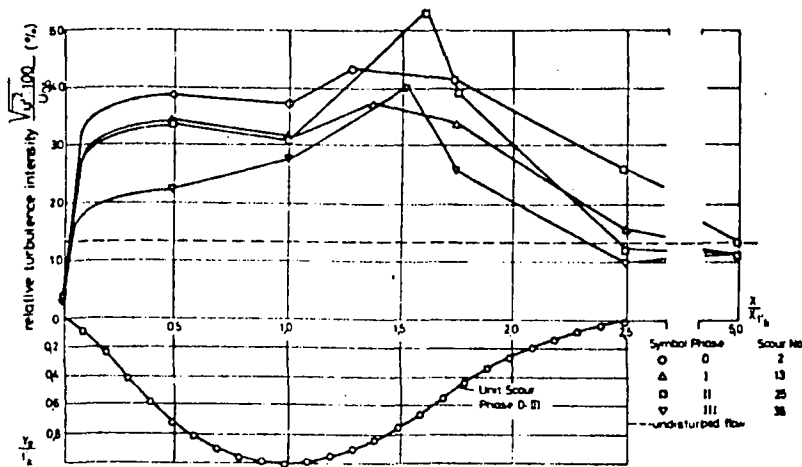
Figure 3-3.   Turbulence intensity and progressive
             scour. /41/

From the studies made by Ahmad, Schoppmann, and Watkins,
it can be understood that the greatest and strongest eddies
have a very big role to play in the development of the scour
hole during the progressive stage. Their observations agree
very well on the location of peak scour activity. What
Schoppmann observed as the point of occurence of peak value
of relative turbulence intensity is in the "region of confused
flow" as termed by Watkins.

3.1.3 Final Stage

The change in an erodible bed configuration because of local
scour results in unsteady flow conditions along the bed. In
general, the enlargement of the flow section results in a
reduction of velocity along the bed, and, therefore, a
reduction in capacity for transport. The rate of scour must
then decrease as the depth of the local scour increases.
Implicit in the above statement is the notion of a limiting
extent of scour. Observations by Schoppmann /41/ completely
agree with this notion. He has found that the turbulence
intensity in scour hole decreases with time - the macroscale
of the turbulence, a measure indicating the size of the
eddies, decreases; that means that the eddies become larger
with increasing scour depths and loose the energy to trans-
port the sediment out of the scour hole.

When the velocities caused by the eddies become equal to the
fall velocity of particles, these particles fall to the bed
again. Thus, this process of lifting bed materials and
rearranging particle size continues, fig. 3-4, till the
vertical velocity gradient, which is very high at the
beginning of the process of development flattens / 2 /;
discontinuity is reduced; eddy intensities increase, so that
lifting of particles is followed by their rolling, and
ultimately the movement stops, attaining a stable condition.
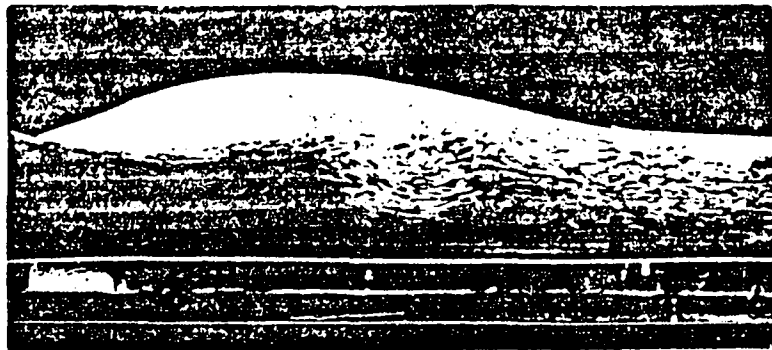
Figure 3-4. Macroeddy in the scour hole. /41/

The scour profile which is the result of the above stated
process consists of two parabolic curves meeting at the
deepest point, see fig. 3-5. / 2 /
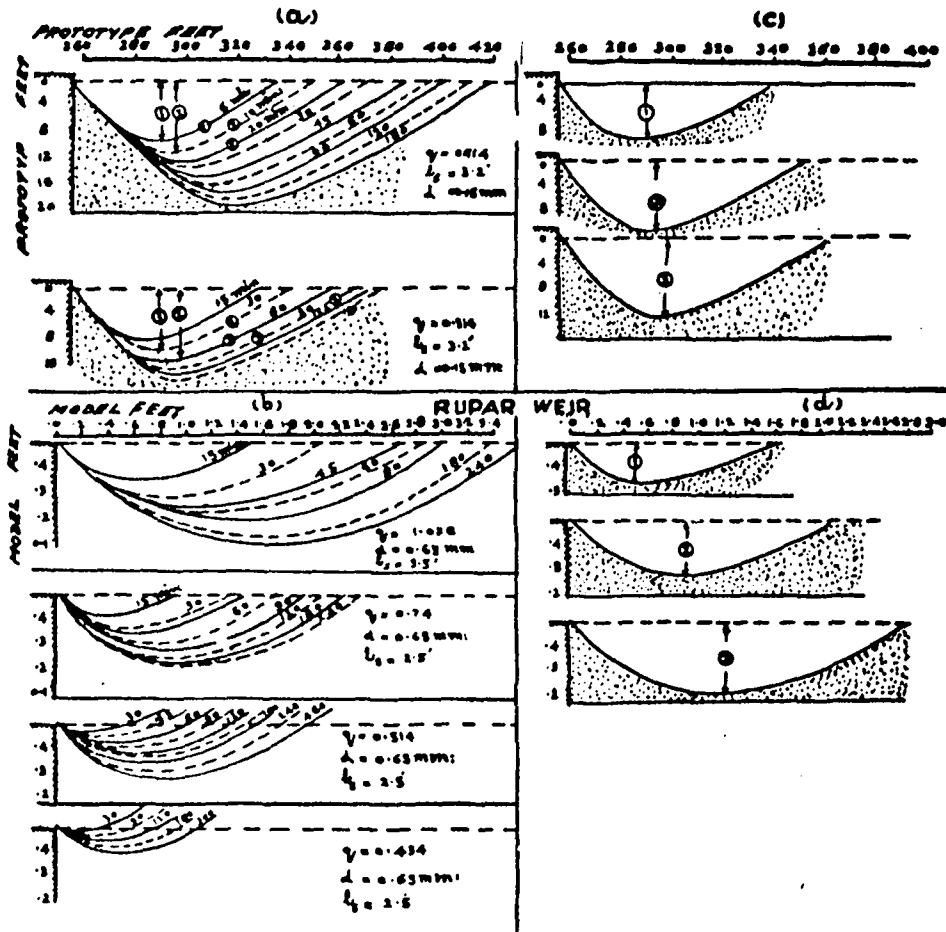
Figure 3-5. Effect of discharge on scour pattern. /2/

3.2 Effect of Water Quality

3.2.1 Clear-Water

Most of the local scour investigations are made for clear-water scour since the scour configuration resulting from the above is more severe than the scour with sediment transport. Information, available on the nature of the latter type of scour is very scanty. However, a detailed experimental investigation comparing the two types of scours was made by De Marchi of Politechnico Milano. His report was published in 1948. Part of the report concerning only the development of scour hole is summerized and included in this and the following section.

a) Free Flow over Weir and Channel Velocity more than the Limiting Value for Sand Carrying /11/

Quick scour occurs immediately downstream of the solid apron at the beginning, with depth and width increasing very swiftly and then the rate of progress becomes slower as the scour hole grows larger. Stable configuration reaches in the upstream part of the scour hole for the short stretch following the solid apron, fig. 3-6, in half an hour.
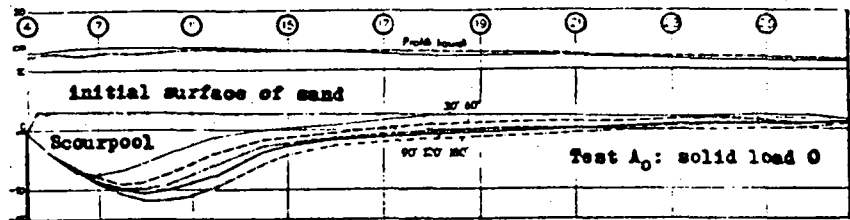
Figure 3-6./11/

Downstream this region scour developed continuously resulting in the intantaneous profiles positioned below the preceeding ones. The cross-section of maximum depth is displaced continuously downstream, see fig. 3-6, as the scour developes with time. This displacement can also be seen very clearly in the experimental results by Schoppmann /41/ presented in fig. 3-7.
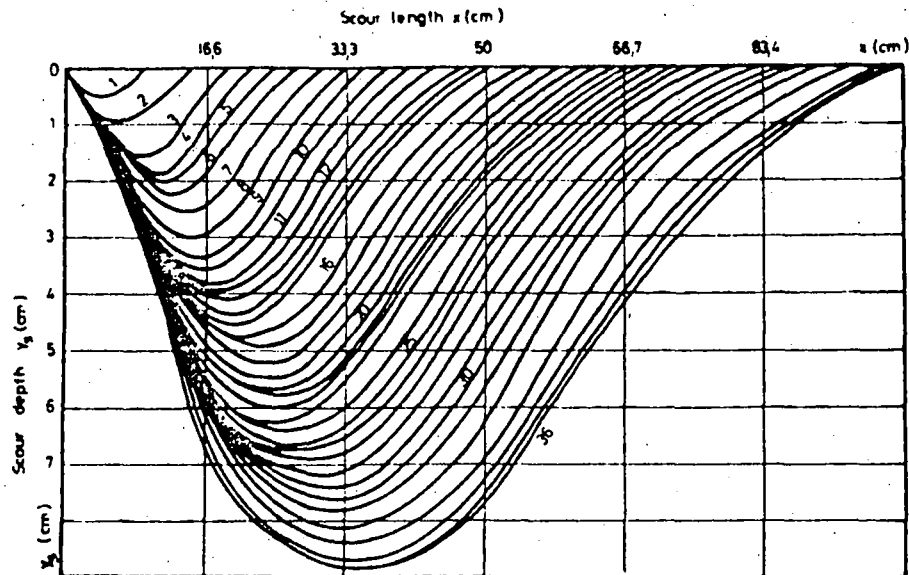
Figure 3-7. Development of scour with time./41/

The scour extends to the channel, downstream of the scour
pool zone, and sand motion in the form of ripples
takes place in the channel.

b) Gate over the Weir Drowned by Raised Tailwater Level
and Channel Velocity Less than the Limiting Value for
Sand Carrying /11/

As the erodible bed following the solid apron is scoured,
the removed sand deposits downstream the scour pool
forming a sedimentation bank (ridge) across the flow.
The ridge so formed grows bigger, the cross-section of
flow at this ridge decreases, and the velocity of flow
increases. When the magnitude of the velocity reaches
the limiting value for sand carrying, wearing away of
the sand deposit commences. De Marchi does not tell
how the process continues at this ridge. However, it
seems reasonable to expect equal rate of deposition and
erosion to proceed continuously.

In the development of the scouring process, a short
stretch of the channel bed affected by alternating
processes of excavation and filling, which are termed
as excavating stage and filling stage, respectively, is
observed. It is learned from De Marchi that
Einwatcher, Nebbia, and some others have observed that
the excavating phenomenon ends abruptly: the sand ceased
to be pulled downstream and began goingd upstream towards
the solid apron with the result of partially filling the
already excavated scour pool. The excavation stage is
associated with a plunged jet and the filling stage with
an undulating jet of flow. These two types of flows are
also occuring alternatingly.

Excavation stages have the same average end configuration
termed as- the excavation profile, fig. 3-8. This result
indicates the existence of a limiting or an end
configuration for local scour dimensions. End configura-
tions of filling stages, termed as filling profiles, show
progressive transformation. The latter are connected with
the profiles of the bank without discontinuity, figure 3-8.
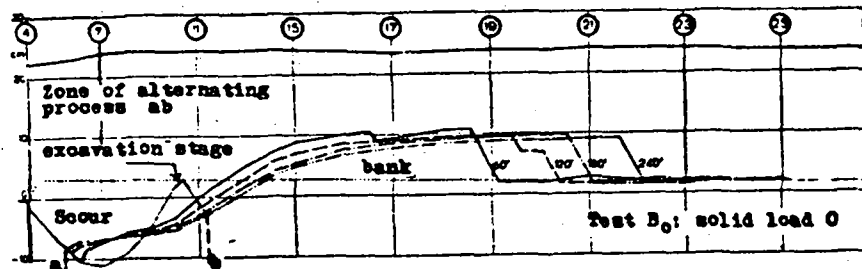
Figure 3-8./11/

As it can be seen in figure 3-8, the alternating process
takes place between cross-sections 6 and 12. In the
upstream region of the scour pool, the bed profile remained
practically unchanged from the first until the fourth hour
of the test. It changes only with type of weir. Downstream
cross-section 12, a progressive deformation of the sand
bank is observed which is characterized by the progressive
stretching of the banks that is maintained by the erosion
of its upper surface. This causes an increase in depth and
a decrease in the velocity of flow of the stream.

According to De Marchi's experimental test results, the
excavation profile for the same test conditions remains
unchanged. This result contradicts the results of latest
investigations carried out by other researchers dealing
with clear-water scour. Many investigators who are studying
the evolution of scour hole dimensions have observed that
there is no a limiting or an end configuration in clear-
water scour.

3.2.2 Sediment Loaded Water

a) Free Flow over Weir and Channel Velocity more than the
   Limiting Value for Sand Carrying /11/

   Local scour with sediment loaded flow is faster in the
   beginning, like clear-water scour, and slows down with
   time. For the same observation interval, the subsequent
   scour profiles in scour with sediment transport are much
   nearer to each other than the profiles in clear-water
   scour observations, and the scour profiles in the former
   type of scour intersect one another as shown in figures
   3-9 and 3-10.
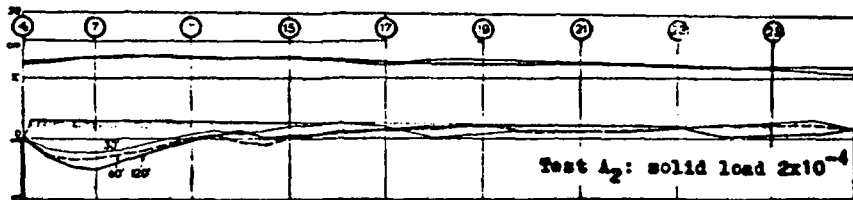
Figure 3-9. /11/
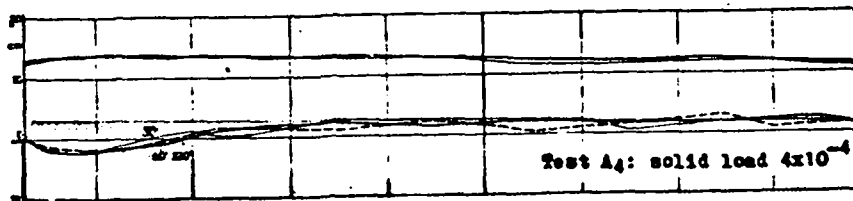
Figure 3-10. /11/

   This leads to the conclusion that certain regions of
   the scour hole which are formed at one stage are refilled
   latter as the process continues. For all other parameters
   kept the same, the size of the scour hole decreases
   with increase of sediment load of the flow.

Figure 3-11 shows scour hole profiles for four different
sediment loads, each obtained after 2 hours run from the
beginning of the test. An interesting thing that must
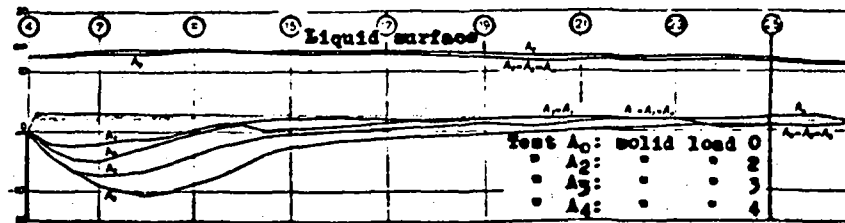
Figure 3-11. /11/

be realized here is that the most undesirable scour
occurs in clear-water scour or in scour with light
sediment load.

A particular feature of the scour with sediment transport
is the formation of a stable average configuration within
some time after the beginning of the process of scour,
which manifests a balance between the supply rate and
the rate of wearing away of sediment. The time taken
to maintain equilibrium is inversely proprotional to
the sediment load of the flow.

In scour with sediment transport, ripples which have
bigger heights than the ripples in clear-water scour
get immediate birth from the scour pool. The movement
of sand, emmited upstream, along the scour pool is such
that it is first deposited at the bottom, downstream
the pool, replacing the sand previously carried away,
and later on this deposited sand is carried away as
far as the channel end.

b) Gate over the Weir Drowned by Raised Tailwater Level
   and Channel Velocity less than the Limiting Value for
   Sand Carrying /11/

At these tests the water velocity is too low to carry
the sand coming out of the scour pool and the sand
is deposited across the flow downstream the scour pool
forming a sedimentation bank which grows higher and higher
in thickness until the velocity of flow above it reaches
such a value which will enable it to erode the surface
of the bank. The upper surface of the bank remains
always higher than the initial surface of sand bed and
it is covered with ripples. The average bank depth
increases progressively in the downstream direction.
Lesser sand volumes are set in motion for higher solid
load. Higher bank thickness is obtained for higher solid
load and the height of the ripples varies also with
solid load. At the most elevated solid load, the bank
acquires a stable configuration and a regimen situation
is reached in the channel.

Similar to the clear-water scouring process, alternating
processes of excavation and filling take place here too.
Excavating phenomenon is ended abruptly 10 minutes
after the beginning of the test and the filling
phenomenon continues until it is replaced by the excavating
phenomenon again. And the alternation process continues
indefinitely. Figures 3-12, 3-13, and 3-14 show profiles
of scour zone for different solid loads. The stretch
between cross-section 4 and 6 is practically the same
for all profiles and coincides with the profile given
by the clear-water scour test.
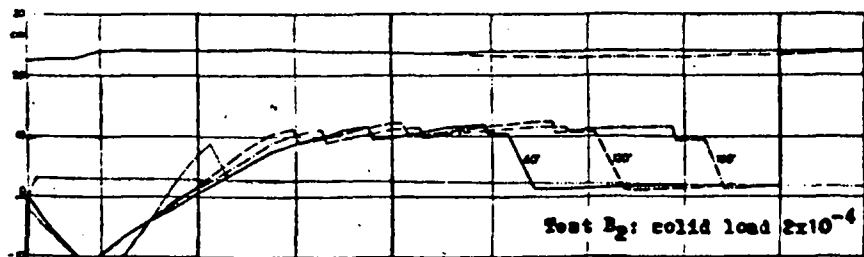
Figure 3-12. /11/
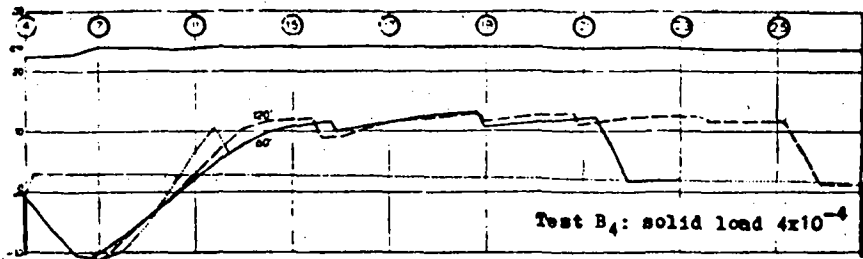
Figure 3-13. /11/
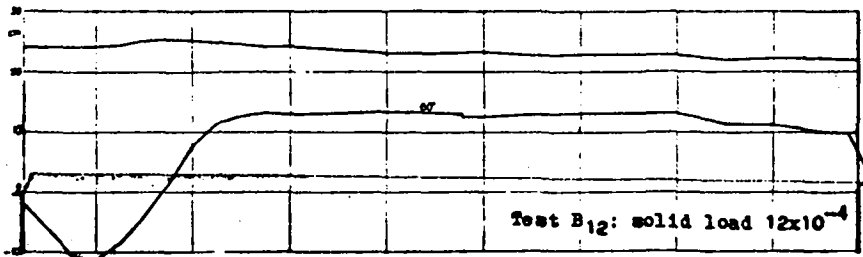
Figure 3-14./11/

Increase of solid load has influences on the duration
of the alternating process, i.e., it prolongs the
excavation stages to about 110 - 130 % of the values
for the clear-water tests and shortens the filling
stages to a few seconds.

4.   SCOUR HOLE DIMENSIONS

4.1   Similarity of Scour Hole Profiles

4.1.1 Method of Evaluation

The common procedure used to check similarity is by plotting
a non-dimensional scour hole profile for every observed scour
hole profile. This is done by choosing one of the characteristic
lenghts (maximum depth of scour is commonly selected) of a
scour hole profile as a repeating variable and dividing the
coordinates which define the scour hole profile by the
repeating variable in order to obtain the non-dimensional
coordinates for the non-dimensional scour hole. Plotting
of these points gives the shape of the non-dimensional scour
hole. All the scour hole profiles are plotted as non-dimensional
scour hole profiles. Similarity is checked by superposing
the resulting profiles. If similarity between the different
scour hole profiles exists, the plotted points will
concentrate along a fixed shape like a parabola with a
vertical axis; otherwise similarity does not exist.

The scatter of the plotted points is a measure of the degree
of similarity. The greater the scatter the lower is the
degree of similarity and vice versa.

4.1.2 Experimental Investigations

Many attemps have been made by researchers to find how closely
similar are the scour hole profiles. Watkins / 50/ and Ahmad
/ 2 / studied scour profiles below solid aprons and the
following investigators studied it below different outlet
structures: Altinbilek and Basmaci / 4 /, Laursen /26/,
Rajaratnam /33/, and Rajaratnam and Berry /32/.

Ahmad carried out three different experiments for different
discharges, different sand grades, and different solid apron
length varying only one of the above parameters in one
experiment. He compared scour profiles of the same maximum
depth in every experiment by superposing them. His report
tells that the profiles of the same maximum depth were exactly
the same in the test results obtained by varying the discharges
and the sand grades whereas profiles of equal depth obtained
by varying the apron length were quite dissimilar. For the
shorter length of apron, the scour profiles were steeper
on both sides of the deepest point and closer to the end
of the solid apron as compared with the longer length of
apron./ 2/

From this study result it can be observed that geometric
similarity should be acquired for the scour hole profiles
to be similar. Ahmad was using a distorted model when he
was changing only the solid apron length of the experimental
set up.

Altinbilek and Basmaci studied the similarity of scour hole
profiles under vertical gates formed by horizontal submerged
jets./ 4 /. The experiments were performed for Froude numbers
1.6 - 24.7 in submerged jet flow, for sediment numbers
3.8 - 13.6, and at varying tailwater conditions.

The non-dimensional profile of the scour hole, obtained by
the above investigators, figure 4-1, is similar to a
vertical axis parabola meeting the plane of a gate.

Altinbilek and Basmaci have plotted also the variation of
the non-dimensional scour hole profile with time, fig. 4-2.
This scour hole profile is geometrically similar as the
development of the scour hole progresses.
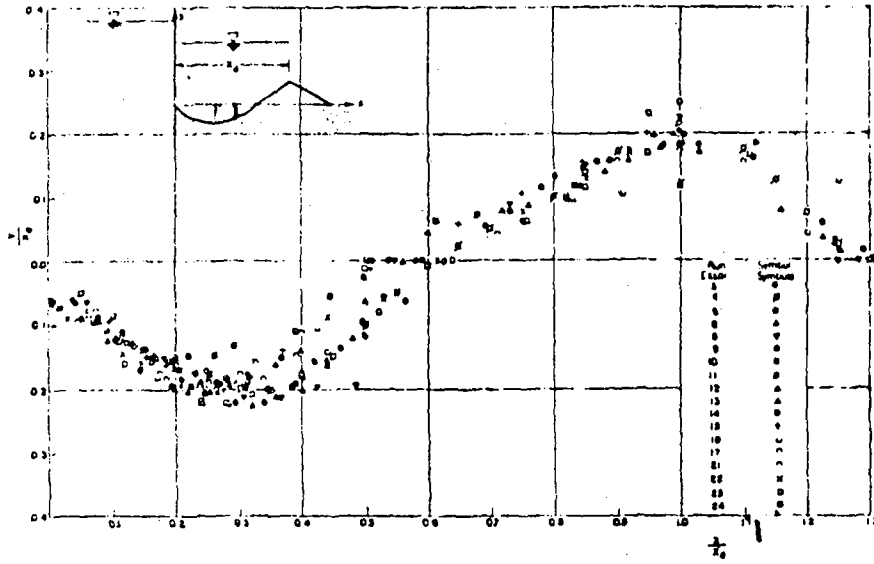
Figure 4-1.   Dimensionless Scour Hole Profile. /4/
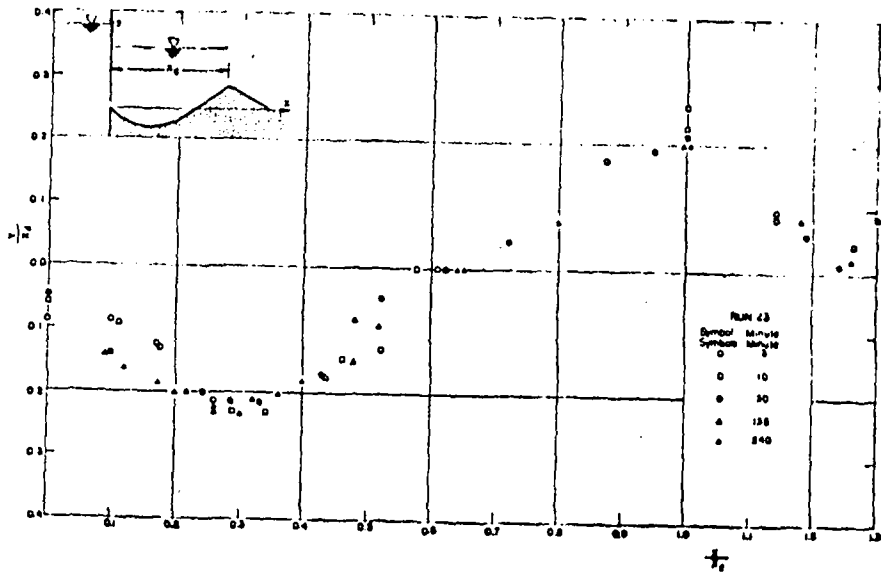
Figure 4-2.   Variation of Scour Hole Geometry with time.
/4/

A similar study as the above mentioned was made by Laursen /26/. He used a submerged jet as the active scouring agent, and varied the flow as well as the bed material characteristics. Sands having the characteristic curves shown in fig. 4-3 were used.

He analyzed similarity of scour hole profiles by plotting the dimensionless coordinates of the profiles as shown in figure 4-4.
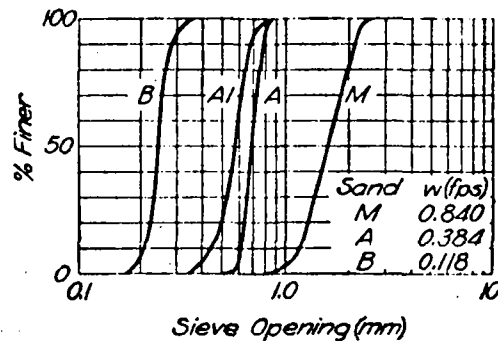
Figure 4-3. Sand Characteristics. /26/
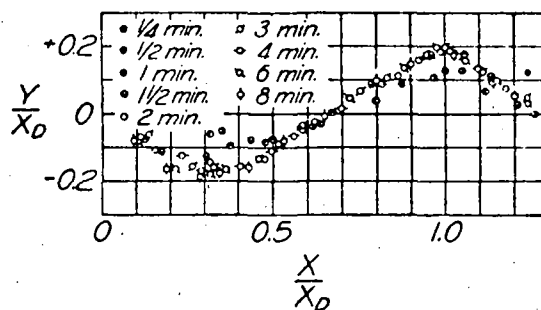
Figure 4-4. Similarity of Scour Profiles. /26/

Laursen has reported that except for the profiles
representative of an initial transitory stage of scour, all
the profiles of a run are superposing. This can clearly be
seen from his plot, fig. 4-4. He has also reported that
the profile forms for all runs of any one sand were almost
identical and the forms for the various sands differed only
slightly.

Rajaratnam, in his study of erosion by plane wall jets with
minimum tailwater /33/, has investigated the similarity of
scour hole profiles. He has used two types of sands with
the mean size D = 2.38 mm and 1.0 mm. In all his experiments
the observtions on erosion were made only after the erosion
profile appeared to have become invariant with time. The
non-dimensional plot of the scour hole profiles is shown
in figure 4-5.
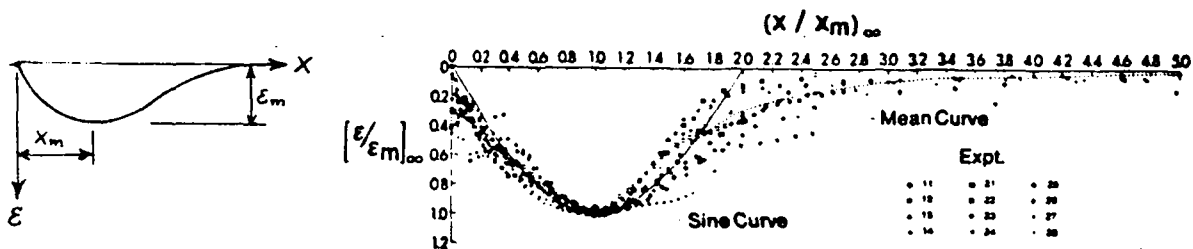
Figure 4-5. Eroded Bed Profiles./33/

The test results by Altinbilek and Basmaci, Laursen, and
Rajaratnam show the existence of an approximate similarity
between scour hole profiles resulting from different discharges
and different bed material types. The above mentioned test
results cannot be compared with each other since the
hydraulic structures obstructing the flow are not
geometrically similar.

From the aforementioned results it appears that the flow
and bed material characteristics have no much effect on the
similarity of scour hole profiles. Probably the effect may
not be significant for the relatively narrow range of values
used in laboratory studies. This, however, may not be
necessarily true for the situation occuring in actual
structures where large hydraulic forces and coarse bed
materials such as gravels, pebbles, boulders, etc. are found.

Watkins has observed the effect of bed material type on
similarity when he made an attempt to find the criteria for
similarity of pot-hole scour profiles /50/. He used the bed
materials shown in table 4-2 in his study and he found that
the criteria for similarity in the pot-hole profile with
the smallest particle size is not closely related to those
with bigger particle sizes. Compared to the type of bed
materials used by the investigators mentioned previously,
Watkins has used a wide range of particle sizes. An important
thing to be noted is that the particle size difference
between the smallest and the next is very big when compared
with the differences between any other consecutive particle
sizes used in his experiment.

From Watkins analyses and the results of the other
investigators it can be deduced that closer similarity occurs
between pot-hole scour profiles in non-cohesive bed materials
with different particle sizes, above a certain limiting
particle size. This limiting particle size is specified to
be 0.5 mm /15/(cited in ref /36/). Flow characteristics which
were also varied in the tests did not show any significant
effect on the similarity of the scour hole profiles.

In the case of scour hole profiles between which similarity
is established, scour hole geometry can be expressed by a
single parameter, namely, the scour depth.

4.2 Length of Scour Hole

Estimation of the length of a scour hole, along the direction
of flow, considering the effects of different cohesionless
bed materials, stream flow characteristics of variable
magnitude acting upon the bed, geometry of the solid apron
and appurtenance structures, and time factor is very useful
for selecting the appropriate method of scour prevention
and protection and for establishing an optimum design
criteria and a suitable construction method for the solid
apron, appurtenance structures, and for the flexible apron.

In this paper, the length of scour hole in an erodible bed
of particle size D should be understood as the measure of
the horizontal distance from a section through the down-
stream end of the solid apron to a section downstream of a
scour hole where the bed material motion impends.

4.2.1 Effect of Bed Material Type

Drag force, lifting force, and stabilizing force are
responsible for the displacement of particles from the
surface of the erodible bed. For every particle the drag
and lift forces are proportional to the projected area of
the particle normal to the direction of flow, and the
stabilizing force is proportional to the volume of the
particle. Since both area and volume are increased with the
increase of particle size, the above forces are increased
in magnitude likewise. The main question, here, should be
the rate of increment of each type of force with respect
to particle size.

Differentiation of the expressions for the forces, eqs. 2.5
and 2.7, with respect to particle diameter gives expressions
for the above mentioned rates of increments.

$$F_{D,L} = C_{D,L} \; K_1 \frac{\rho U^2}{2} D^2 \qquad (2.5)$$

$$F_g = (\rho_s - \rho) K_2 D^3 \qquad (2.7)$$

Now,
$$\frac{dF_{D,L}}{dD} = C_{D,L} \; K_1 \; \rho U^2 D \qquad (4.1)$$

and,
$$\frac{dF_g}{dD} = 3 \; (\rho_s - \rho) \; K_2 D^3 \qquad (4.2)$$

Comparison of eqs. 4.1 and 4.2 reveals that the rates of increment of $F_{D,L}$ and F_g are proportional to D and D^2, respectively. This implies that if all other factors, at a cross-section of a scour hole, are kept constant and only D is changed, a condition can be found where all the forces are in balance for a certain value of particle size D, which may be termed as the limiting D. At such a cross-section, scour proceeds in a bed material which consists of particles of diameter less than the limiting D, and no scour otherwise.

For the same upstream condition, the flow characteristics at different cross-sections of an erodible bed are also normally different. Among other characteristics, the macro turbulence intensity varies along the bed. It increases with the increase of length from the downstream end of the solid apron in the flow direction, see figure 4-6.
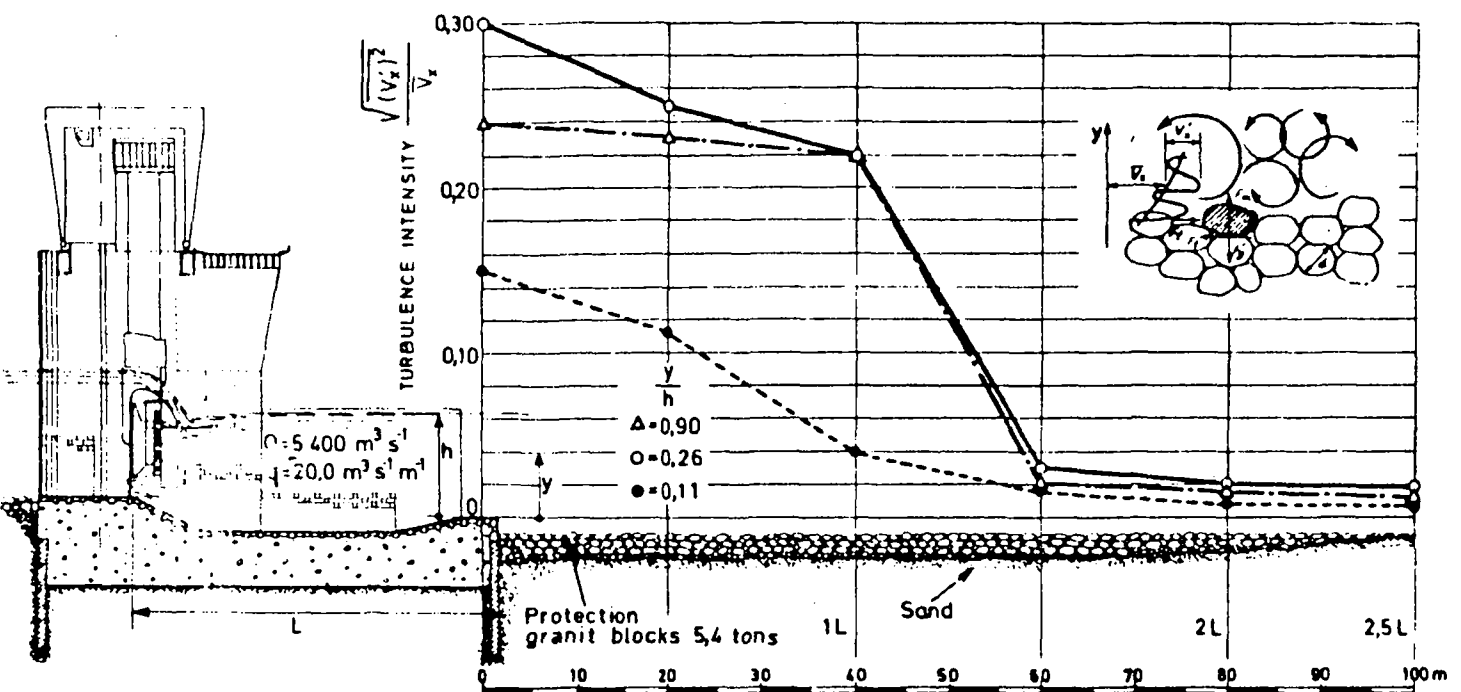
Figure 4-6. Macroturbulence intensity downstream the stilling pool./38/

Macroturbulence is associated with fluctuation of local velocity /51/. The intensity of macroturbulence is a measure of scouring capacity of the flow. A decrease in macro-turbulence intensity is a decrease in scouring capacity. This can be verified by the distribution of maximum instantaneous near bottom velocity which is decreasing in the downstream direction /28/ as shown in figure 4-7. It decreases until it reaches the magnitude of the velocity for the channel flow.

F_{z_1}	15,4	26	37,8	40			52		71,3
h_y/h_n	1,30	1,24	1,62	1,03	1,27	1,74	1,1	1,39	1,23
	◊	△	⊙	◓	∅	◪	□	+	+

$$\frac{U_A^*}{V_2}$$

$F_{z_1} = 75$

$F_{z_1} = 50$

$F_{z_1} = 25$

$$\frac{x}{h_2}$$
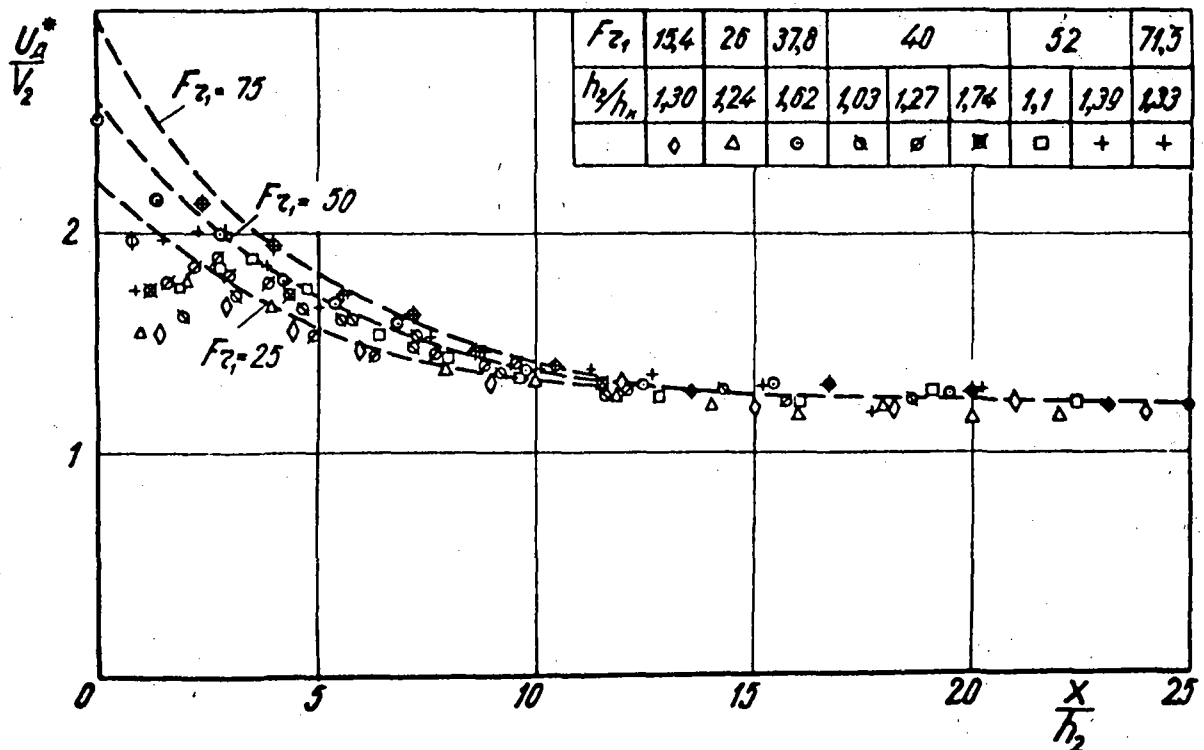
Figure 4-7.   Variation of U_A^*/V_2 along the flow length
below the stilling basin./28/

In figure 4-7 ,

U_A^* = maximum instantaneous near bottom velocity,

V_2 = average velocity of flow at the section
following the hydraulic jump ,

x = distance from solid apron end to investigated
section ,

h_2 = sequent flow depth.

The destabilizing force responsible for the local scour
decreases with decrease of the maximum instantaneous near
bottom velocity until the latter attains the bed velocity
for normal channel flow.

The interacting forces are in balance at the end of the
scour hole length. For different particle sizes used as bed
material, there will be different sections where the above
situation occurs. The section for a smaller particle size

has to be downstream of the section for a larger particle
size. Thus, the length of scour hole has to increase with
the decrease of particle size of the bed material.

The above concept is in complete agreement with the
investigation results whose literaure is available at
the moment.

From model tests for Jaba level crossing /2/, to determine
the shape of eroded profile variation with different
particle size bed materials, the result shown in figure
4-8 is obtained.

To compare the scour lengths in different particle sizes
of bed material, table 4-1 is made for the particular
situation of the solid apron length, $l_s = 0.98$ m ($=3.2$ ft),
discharge intensity, $q = 0.020$ m^3/s m ($= 0.27$ ft^3/s), and
duration of scour in minutes, $t = 15$, 30, 45, 60, 90, 120,
and 150. These tabular values clearly show that for the
same duration of scour, the scour length is smaller in bed
materials of larger particle size, and vice versa.

Table 4-1. Scour lenghts in different particle sizes
of bed material.

Particle diameter D (mm)	Scour hole length from the end of solid apron in m (ft)						
	Durations in minutes						
	15	30	45	60	90	120	150
0.15	30.0	33.2	38.7	42.1	44.5	46.3	47.2
	(95)	(109)	(127)	(138)	(146)	(152)	(155)
0.42	24.1	30.5	33.5	36.3	39.0	41.8	43.0
	(79)	(100)	(110)	(119)	(128)	(137)	(141)
1.12	22.6	28.7	32.0	35.1	37.5	39.3	42.1
	(74)	(94)	(105)	(115)	(123)	(129)	(138)
2.24	18.9	24.4	29.0	29.9	31.7	–	–
	(62)	(80)	(95)	(98)	(104)	–	–
3.33	14.0	16.2	17.7	18.6	19.5	21.3	–
	(46)	(53)	(58)	(61)	(64)	(70)	–

Table 4-2 shows the materials used in the test and their properties. /50/

Table 4-2. **Bed Material Properties**

Material No.	Particle Sizes			Spec. Grav.	Fall Velocities			Repose Slope	V_o ft./sec.	Notes
	Sieve Limits		d		Limits		s			
	in.	in.	in.		ft./sec.	ft./sec.	ft./sec.			
S	0.011	0.023	0.017	2.65	0.12	0.21	0.17	1 : 1.65	0.6 ±0.1	River sand
G1	⅟₆₄	⅟₁₆	0.14	2.64	0.77	0.89	0.83	1 : 1.25	2.0 ±0.2	River gravel
G2	⅟₁₆	⅟₁₆	0.25	2.63	0.95	1.27	1.11	1 : 1.25	2.8 ±0.2	River gravel
G3	⅟₈	⅜	0.44	2.65	1.09	1.57	1.33	1 : 1.15	3.0 ±0.3	River gravel
G4	⅛	¾	0.63	2.65	1.23	1.85	1.54	1 : 1.05	3.5 ±0.5	River gravel
M	0.011	0.7	0.3	2.65	0.12	1.85	1.0	1 : 1.05	1.5 ±0.5	Mixture of equal parts by weight of S, G1, G2, G3, G4
L	⅛	⅞	0.65	1.54	0.91	1.25	1.08	1 : 1.25	2.2 ±0.2	Pellets of expanded shale aggregate
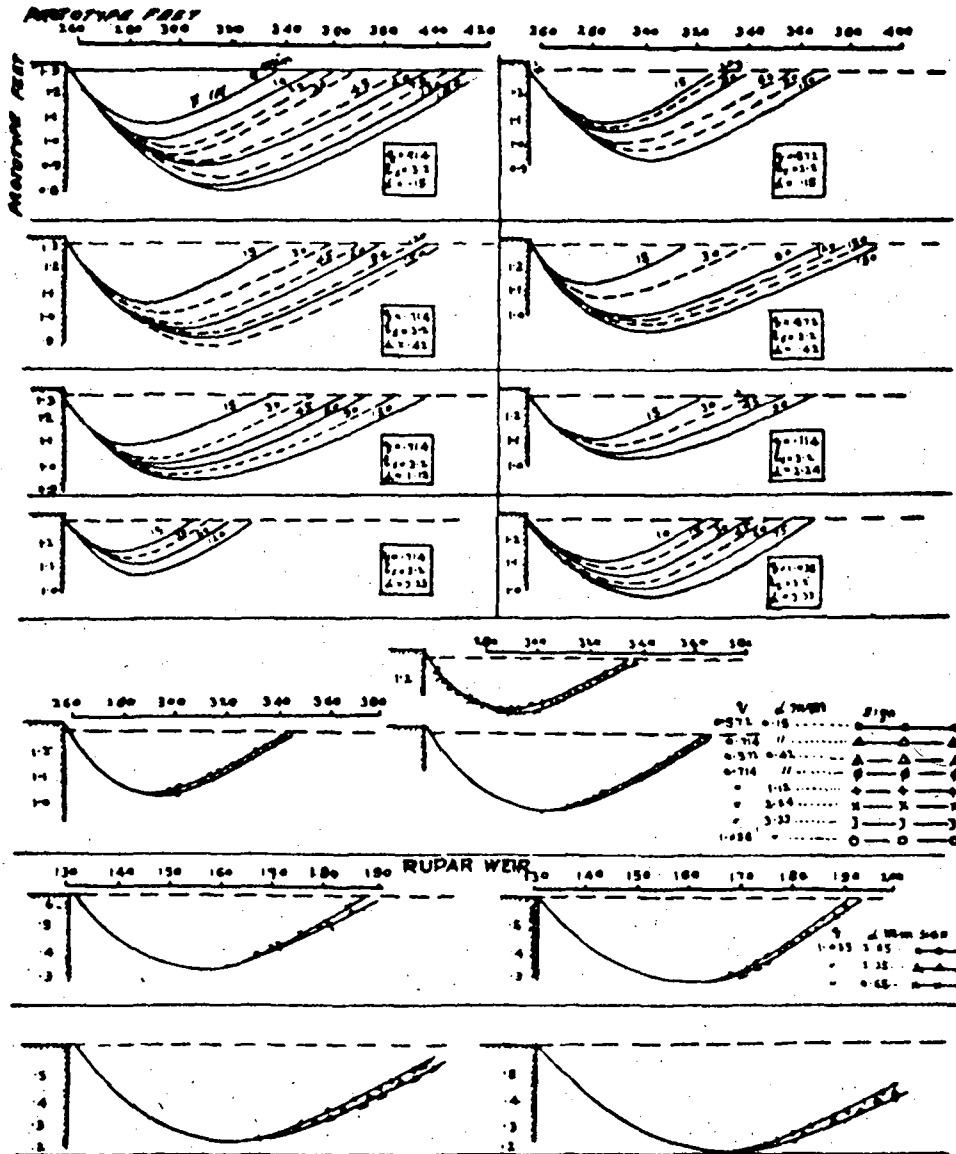
Figure 4-8. Effect of size of sediment on scour pattern./2/
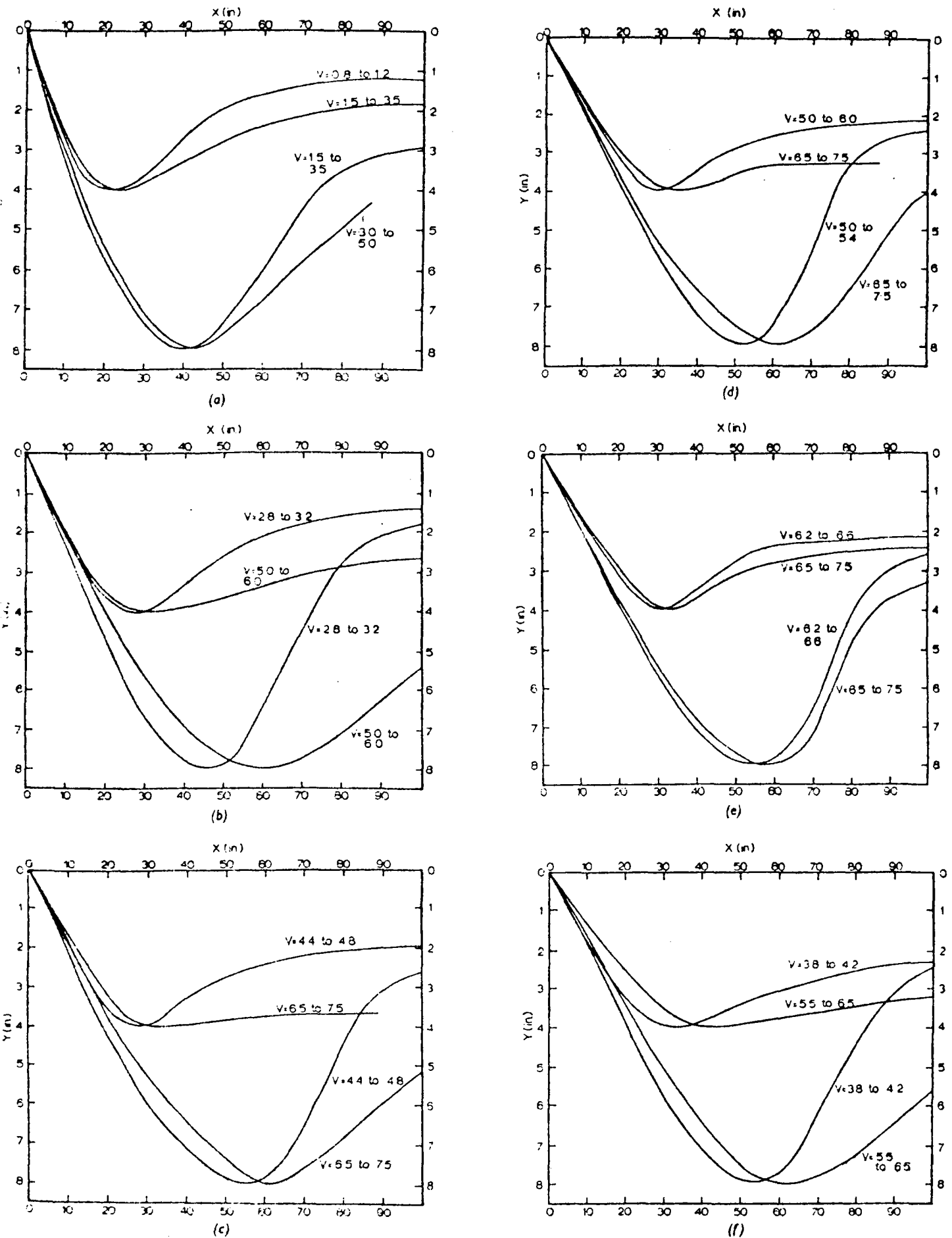
Figure 4-9. .—*Scour Profiles in Bed Materials.* /50/

(a) Material S   (d) Material G3
(b) Material G1   (e) Material G4
(c) Material G2   (f) Material L

The curves in figure 4-9 indicate the bed profiles which occured in different bed materials owing to stream flows of various magnitudes obtained from experimental investigation result by Watkins./50/

Each curve in figure 4-9 represents the average of the band of scour profiles which occured with a stream jet velocity within the range of values marked alongside the curve. Two pairs of profiles, shallow and deep, are presented for each type of bed material. All the shallow profiles are obtained for one and the same maximum scour depth and the deep profiles for another and also the same.

Superposing the scour profiles in the materials G_2, G_3 and G_4, for the velocity range of V = 1.98 - 2.29 m/s (= 6.5 - 7.5 fps), figure 4-10 is obtained.
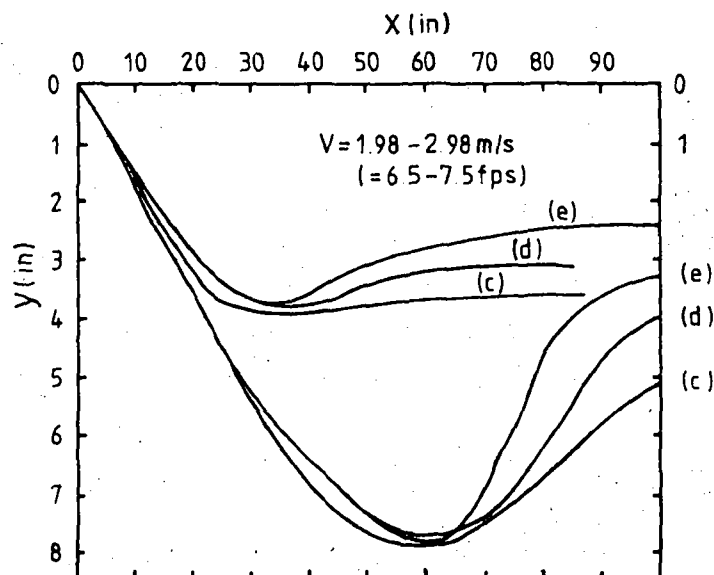
Figure 4-10. Scour profiles of the same maximum depth in bed materials of different particle sizes. (After Watkins /50/)

Observation of the scour hole profiles downstream of the
maximum depth in figure 4-10 shows that the profile in a
bed material of larger particle size is located at a lower
elevation than the profile in the bed material of smaller
particle size.

Assuming the velocity for impending motion of each type of
bed material is greater than the bed velocity of the normal
channel flow following the scour hole, and based on the
relative location of the scour profiles in figure 4-10,
it is possible to conclude that the scour profile in the
bed material of bigger particles will reach the original
bed level at a shorter length than the profile in the bed
material of smaller particles.

From the available test result reports and the above analysis
it can be clearly seen that for the scour profiles formed
in bed materials of particle sizes under similar conditions
of test, the length of scour hole formed at the same
elevation is bigger in relatively smaller particles, and
vice versa. However there is no an established general
formula to estimate the length of a scour hole expected in
a bed material, or to relate scour lengths in different
materials. One has to resort to experimental investigation
whenever a need arises.

Knowledge of the expected length of local scour in a bed
material of particular particle sizes is very important in
the design stage either to allow for the scour to occur or
to provide reliable protection.

4.2.2 Effect of Apron Length

There are no many investigations done to determine the
effect of solid apron length on the development of scour
hole length. The only report that could be available is due
to Ahmad /2/. It includes the effect of different apron
lengths below the hydraulic jump, on the shape of eroded
profile. Comparison of the results, shown in figure 4-11,
for the same duration and different apron lengths, 1_s,
indicates the increase of scour hole length with the
decrease of solid apron length.
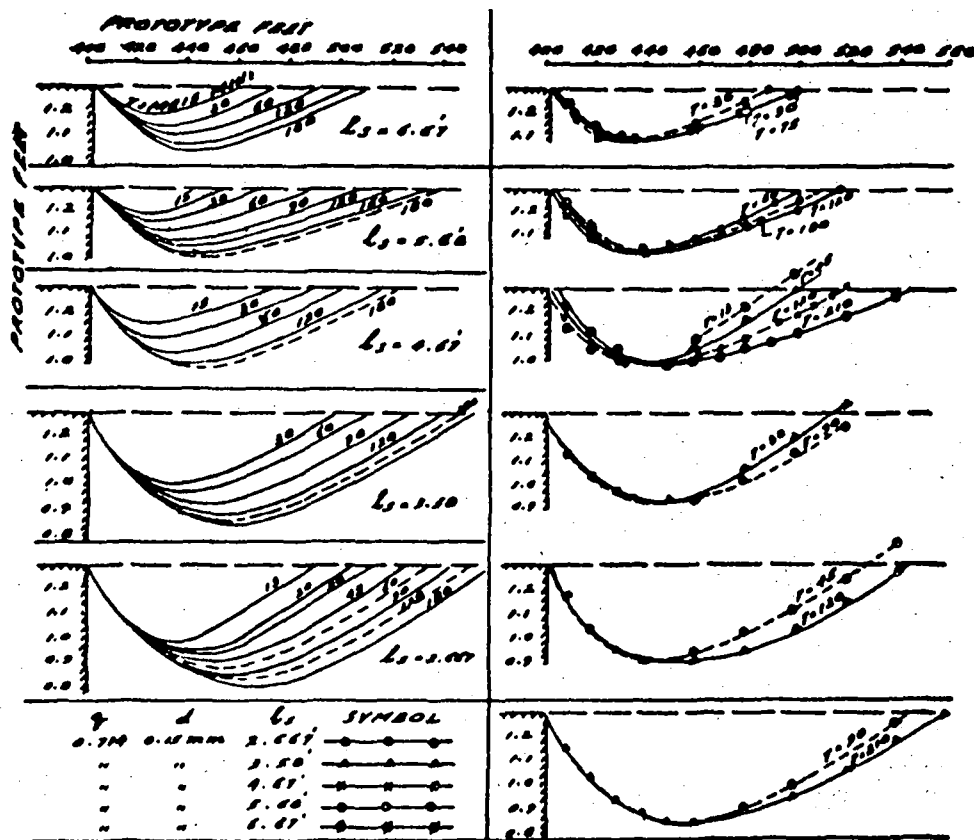
Figure 4-11. Effect of 1_s on scour pattern./2/

The result appears reasonable since the zone of flow
tranzition (the region from the end of hydraulic jump
length to the section downstream where normal channel flow
is restored), in contact with the erodible bed, will be
longer when the solid apron length is made shorter. In
this region of contact of the erodible bed with the flow,
local scour takes place due to the prevailing macroturbulent
flow.

4.2.3 Effect of Appurtenance Structures

4.2.3.1 End Sills

Observation of results of investigations made to determine
scour profiles, reveals the increase of scour length when
end sill are provided./9/37/

In figure 4-12 are shown four different types of sills
used in a model investigation and the scour hole profile
corresponding to each type of end sill /37/. Sill type 2
approaches, in shape, a horizontal apron without sill. The
length of scour hole corresponding to it is relatively
shorter than the other shapes. From this result, it may
not be wrong to imagine the shortest scour hole length to
correspond to a horizontal solid apron without sill.
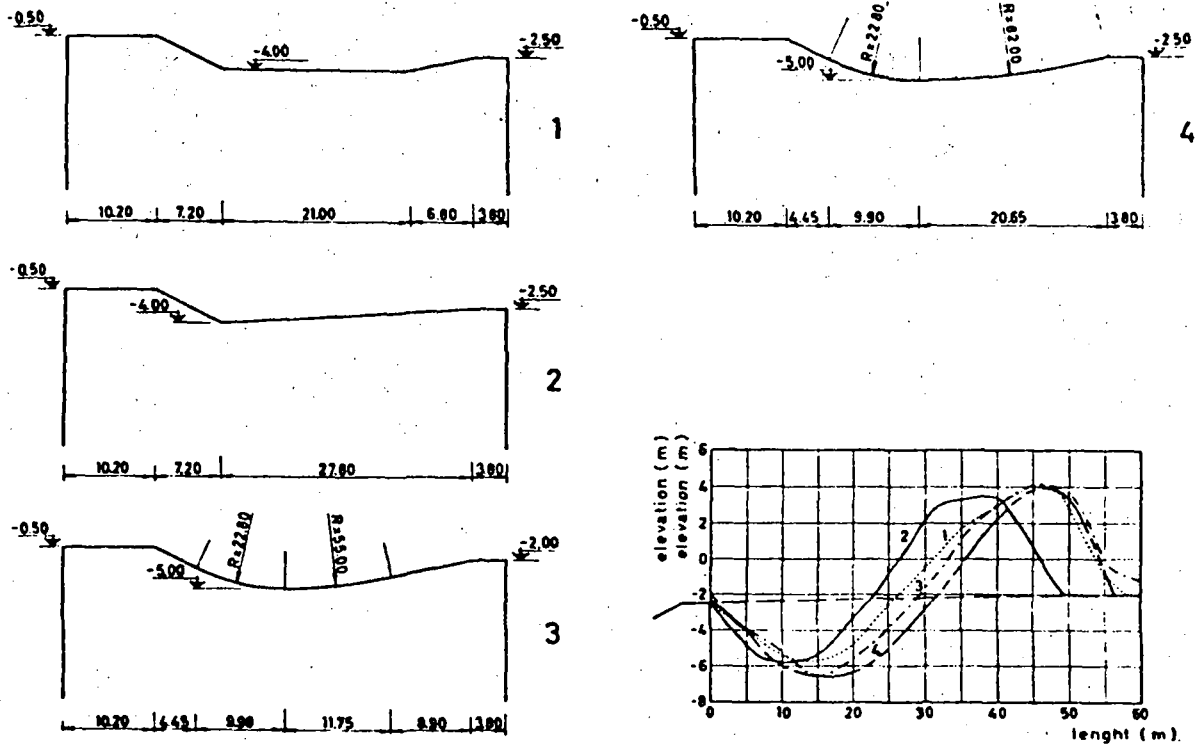
Figure 4-12. Crestuma dam: sills and erosion profiles./37/

Experimental test results by Catakli et al /9/ on scour
shapes resulting from stilling basins without sills and
stilling basins with sills of different sizes but the same
shape indicate that the scour lengths with sills are longer
than those without sills. This can be analyzed from the
empirical equations they developed by considering the scour
hole profile as parabolic. See figures 4-13(a) and 4-13(b).
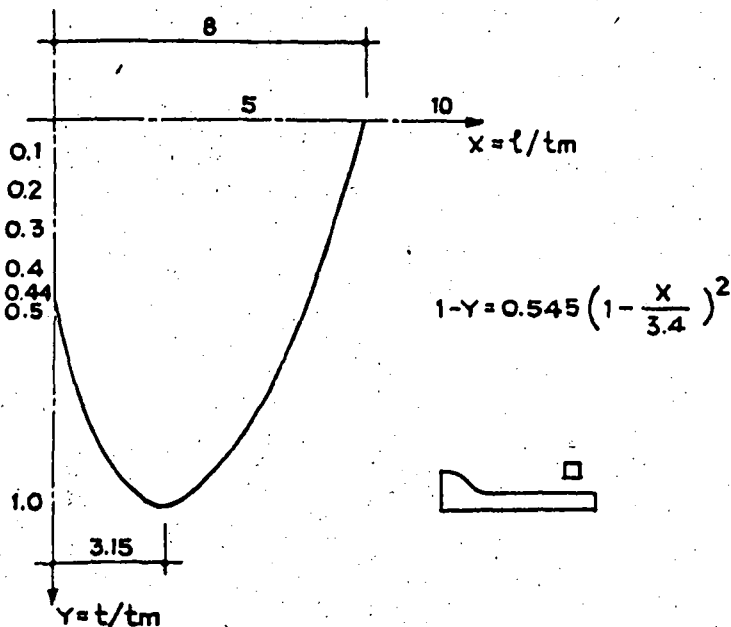
$$1-Y = 0.545\left(1-\frac{x}{3.4}\right)^2$$

Figure 4-13(a).

The average scour form
for the stilling basins
with beams but without
end sill./9/

$$1 - Y = 2.35 \left(1 - \frac{x}{10.5}\right)^2$$
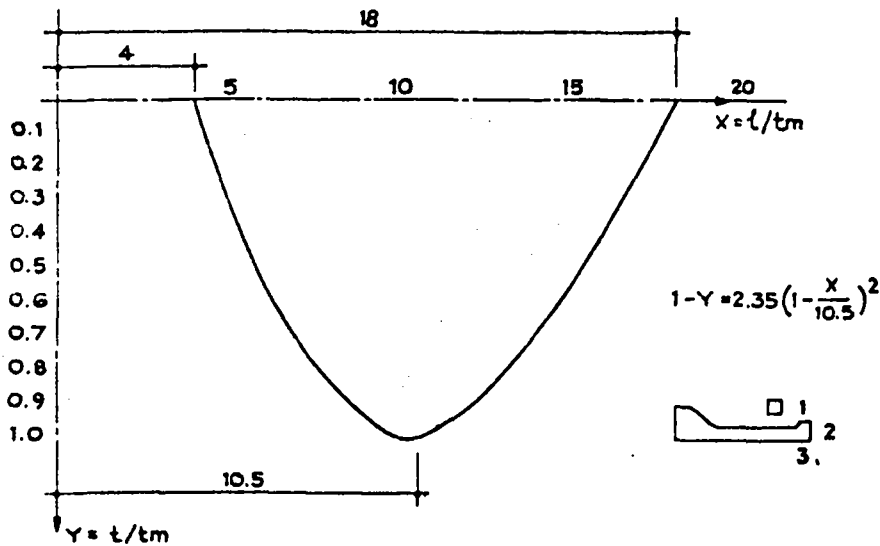
Figure 4-13(b).   The average scour form for the stilling
basins with sill and beams./9/

A definition sketch of the experiment is given in figure
4-14.

Denoting $t/t_m = y$, $1/t_m = x$,

they expressed scour profile by

$$1 - y = C_1 \left(1 - \frac{x}{C_2}\right)^2 \qquad\qquad (4.1)$$

Without sill : average $C_1 = 0.552$, $C_2 = 3.28$
With sill: average $C_1 = 2.30$, $C_2 = 10$, for
             $h'/h_2 = 0.10 - 0.20$

Rearranging equation 4.1 gives,

$$x = C_2 \left(1 - \sqrt{\frac{1-y}{C_1}}\right) \qquad\qquad (4.2)$$

At the ultimate stage of scour development $t = t_m$ and
$y = 1$. Therefore $\sqrt{\frac{1-y}{C_1}} = 0$ in equation 3.2. This gives as
a final result

$$x = C_2 \colon \text{ i.e., } \frac{1}{t_m} = C_2$$

or $1 = t_m C_2$.
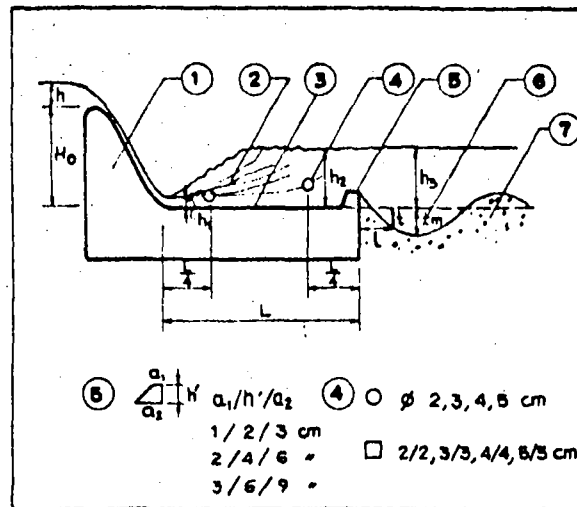
Figure 4-14.   Spillway, stilling basin and scour form. /9/

(1) Spillway.   L   Length of stilling basin.
(2) Hydraulic jump. h_1 First depth of hydraulic jump.
(3) Apron (Stilling basin). h_2 Second depth of hydraulic jump.
(4) Horizontal beam. h_3 Tail water depth.
(5) End sill. t_m Max scour depth.
(6) Scour Form. t Scour depth, at the distance of l.
(7) Flow bed material. l Scour distance from end of stilling
H_0 Spillway height.   basin.
h Water nappe height.

For stilling basins without sill: $l = 3.28\ t_m$.

For stilling basins with sill: $l = 10\ t_m$.

The relative values for t_m can be estimated from the following empirical formula developed by the same investigators:

$$t_m + h_2 = K\frac{q^{0.6}(H_0+h)^{0.2}}{(d_{0.90})^{0.1}} \qquad (4.3)$$

where

  q = discharge intensity, $m^3/s\ m$

  $d_{0.90}$ = particle size of bed material 90 % of which is finer, mm

  K = form factor.

For the same conditions of test in stilling basins without and with sill, $t_m = f(K)$.

K   values: for stilling basin without sill   =   1.614
               for stilling basin with 2/4/6 sill=   1.531 /9/

Now, the relative values of scour hole length, 1_r, can be estimated:

for stilling basin without sill: 1_r = (3.2)(1.614)

$$= 5.29$$

for stilling basin with 2/4/6 sill: 1_r =(10)(1.531)

$$= 15.31$$

Thus, the scour hole length with sills is about three times the length without sills.

It has to be remarked here that as stated by the investigators of the above test, using sill at the end of solid apron may cause the scouring to start $4t_m$ away from the stilling basin, see figure 4-13(b). But in the case without sill, scour begins at 0.4 t_m from the bottom, figure 4-13(a).

4.2.3.2 Baffle Piers

An intensive study with a series of experiments has been done by Framji on a model called "Kotri Barrage Model", to determine the scour below the barrage, with and without baffle piers. Comparison of contours of scour holes without baffle piers and with two rows of staggered baffle piers manifests the effect of baffle piers in reducing the scour hole length./15/

From their studies of a flat stilling basin without any energy dissipator and a series of studies with eight different arrangements of baffle piers, figure 4-15, Zimmermann and Maniak have reported that the dimensions of the scours were reduced by more than 50 % when baffle piers were provided./53/
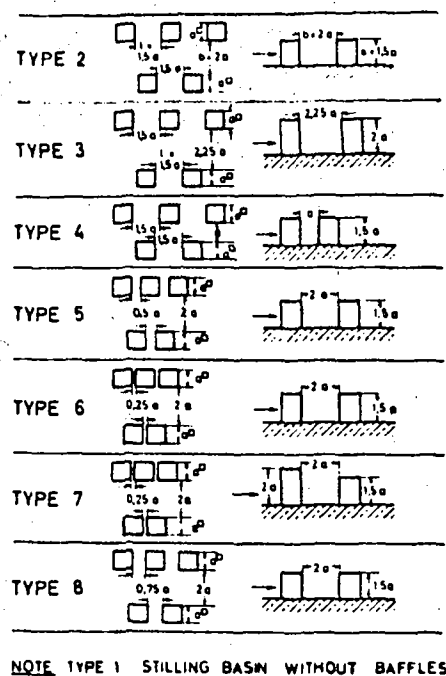
Figure 4-15. Types of baffle piers./53/

Within the limitations of the design elements of baffle piers, specified in their test, the above investigators have arrived at an empirical relationship, eq. 4.4, to estimate the approximate length of scour hole, l_K, when the maximum depth, t_K, of the latter is known./53/

$$l_K = 10.7 \, t_K, \text{ (m)} \tag{4.4}$$

An arrangement of baffle piers according to type 4, figure 4-15, showed a reduced length of

$$l_K = 9.2 \, t_K, \text{ (m)} \tag{4.5}$$

The value of t_K is estimated from the relationship

$$\frac{h_2 + t_K}{(\dfrac{h_2}{g^{2/3}})^{0.93}} = \frac{2.89 \, q^{0.82}}{(d_{85})^{0.23}} \tag{4.6}$$

where,

h_2 =   depth of tailwater, m

q   =   discharge intensity of wier, m^3/s m

t_K =   depth of scour, m

d_{85} =   the particle size for which 85 % of the river bed material is finer.

Regarding a stilling basin without any special energy dissipators, the length of scour hole, within certain limitations, is estimated by

$$5 \ t_K \leq l_K \leq 7 \ t_K \quad /53/ \qquad (4.7)$$

and t_K is obtained from

$$\frac{h_2 + t_K}{(\frac{h_2^{0.73}}{g^{2/3}})} = 2.23 \frac{q^{0.72}}{(d_{85})^{0.08}} \qquad (4.8)$$

Note: The same value of t_K cannot be used to compute the scour lengths in equations 4.4 and 4.7.

4.2.3.3 Chute Blocks

Chute blocks improve the performance of a jump (sec. 6.1.1.2). When the performance of a jump is improved, it is natural to expect a reduction in the scouring capacity of the flow leaving the jump floor. However, in a model test made by Suryavanshi et al /43/, to determine the use of chute blocks in stilling basin for Tawa Dam (India), it is revealed that the provision of chute blocks increases the energy dissipation as well as the scour size, see figure 4-16. The two results appear contradictory. The explanation given by the investigators is that an inspection of the flow pattern at the end of the stilling basin in the two cases, with and without chute blocks, figure 4-7, would reveal that the

maximum velocities existing in the basin without chute
blocks have a tendency to prominantly throw away the jet to
the surface and a small return flow is observed when the
chute blocks are absent. They have mentioned in their
report that the increase in scour with addition of chute
blocks is also announced by Roorkee Research Station.

It appears unwise to incur extra expense by providing chute
blocks if the main purpose is defeated. However, chute
blocks may have an influence on the reduction of the impact
load on the stilling basin floor. It is not the scope of
this paper to discuss the latter. Nevertheless, if it could
be found that chute blocks do not also serve to reduce
impact load of the stream on the basin floor, they must be
avoided altogether.
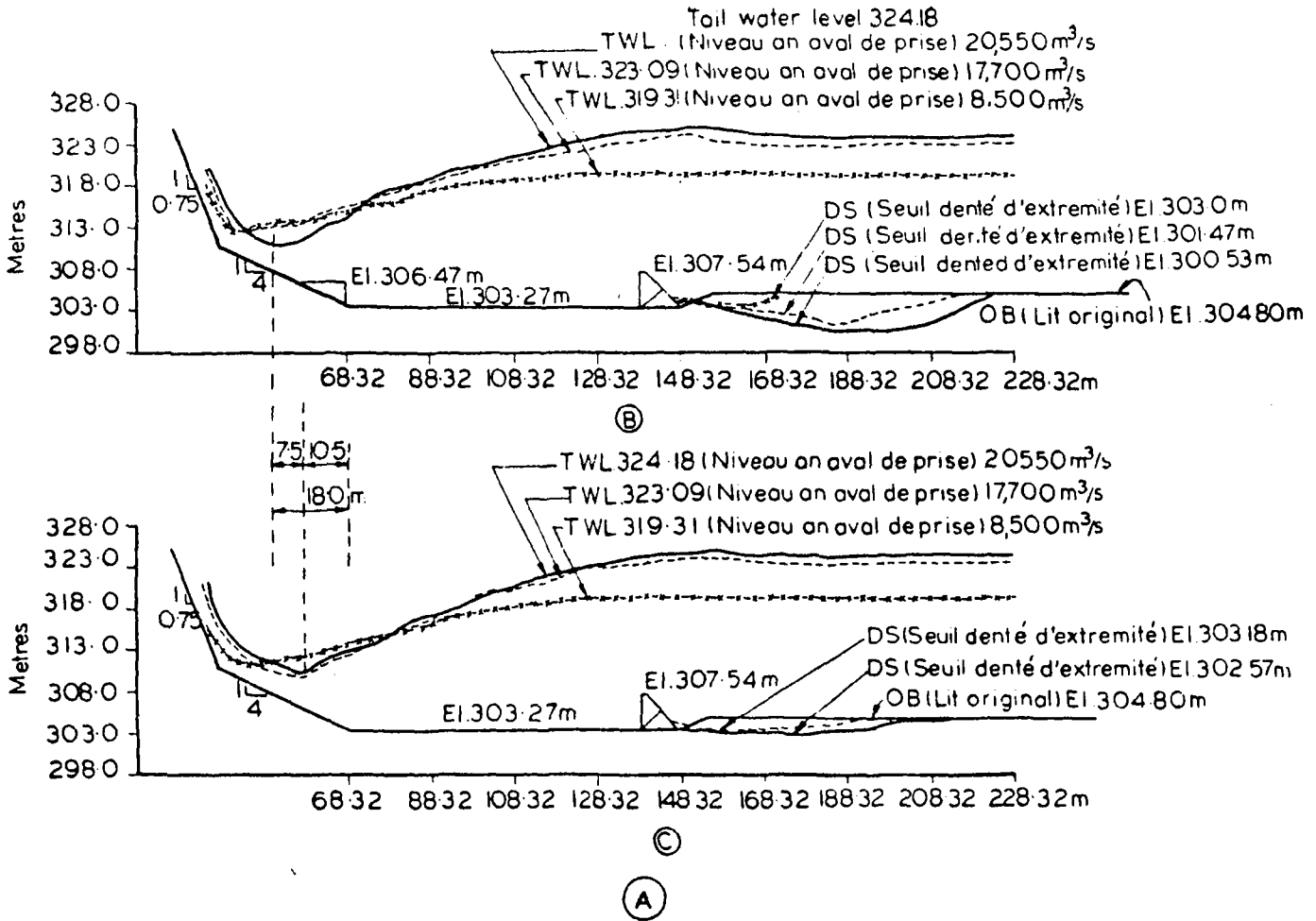
Figure 4-16./43/

(A) Stilling basin observations. Tawa Dam
     Models.
(B) With chute blocks.
(C) Without chute blocks.
(El) Elevation.
(D.S)Deepest scour.
(O.B)Original bed.

(a) Discharge 20,550 m³/s
(décharge 20,550 m³/s)

Tail water level 324 18m
(Niveau en aval de prise)

(b) Discharge 17700 m³/s
(décharge) 17700 m³/s

Tail water level 323 09m
(Niveau en aval de prise)

(c) Discharge 8500 m³/s
(décharge) 8500 m³/s

Tail water level 319 31m

(A) Fig. 5
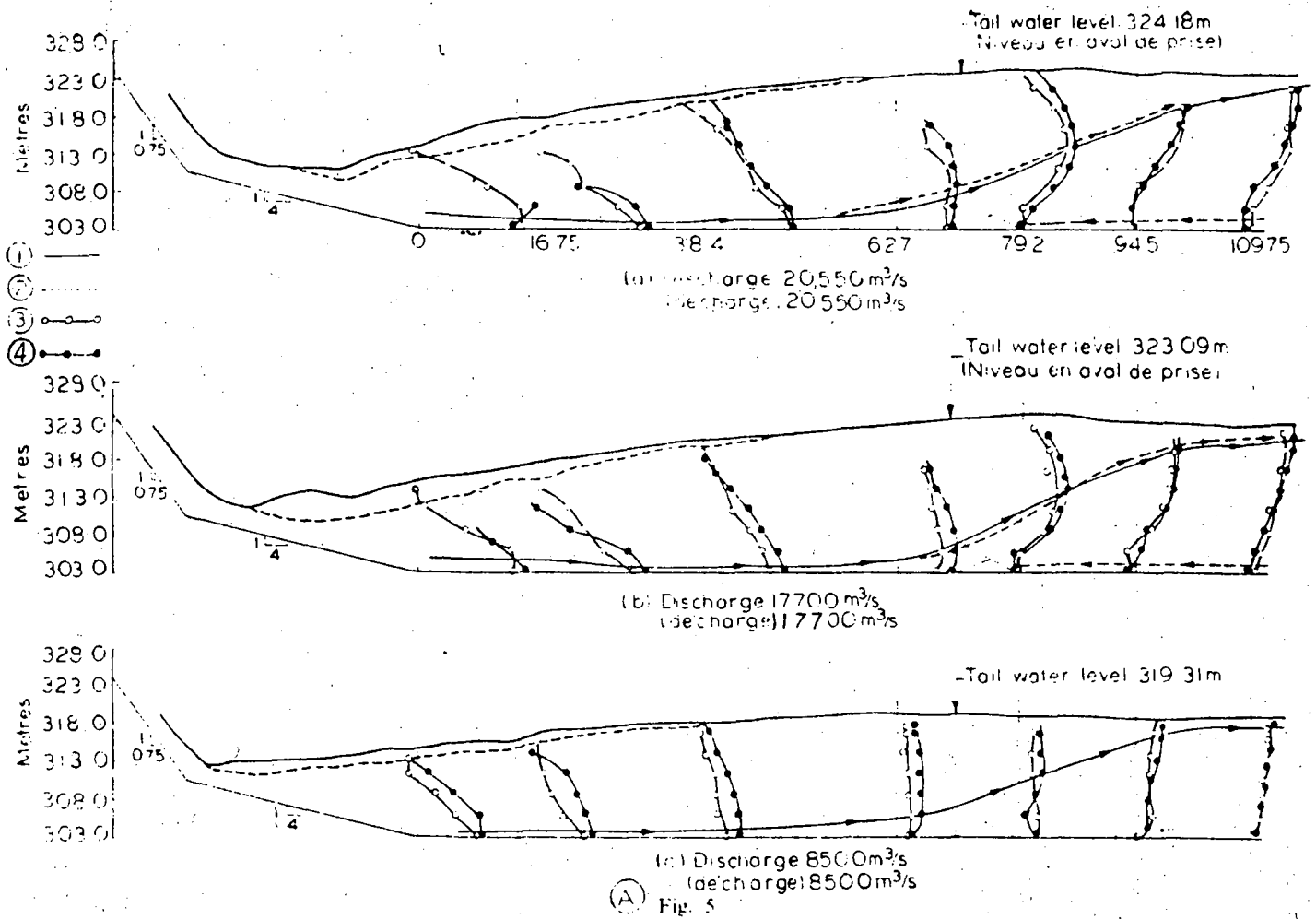
Figure 4-17./43/

(A) Velocity distribution with and without chute blocks.

1. Water surface profile with chute blocks.
2. Water surface profile without chute blocks.
3. Velocity distribution with chute blocks.
4. Velocity distribution without chute blocks.

4.3 Depth of Scour Hole

By depth of scour hole, it should be understood as the instantaneous maximum depth of the scour hole profile measured from the original bed level to the deepest point of the profile. When the scour activity decreases with time and becomes insignificant the scour hole profile stabilizes. The resulting maximum depth of scour is termed as the ultimate depth of scour. This is the most important dimension which is used to decide whether the scour has to be allowed or protected.

The factors influencing the depth of scour hole are dealt within the following sections. These factors are bed material type, dimensions of stilling basin and appurtenance structures, and flow characteristics.

4.3.1 Effect of Bed Material Type

In most of the empirical equations developed to estimate the terminal depth of scour holes, one of the factors involved is the grain size of the bed material. Some of such empirical equations are given below:

Equation 4.9 is developed by Lacey /15/ (cited in ref. /25/):

$$D = 0.9(g^2/f)^{1/3} \qquad (4.9)$$

where,

D = normal depth of flow for regime condition, ft

g = discharge intensity, cusecs/ft

f = Lacey's silt factor which for regime condition approximates to 1.76 m, approximately, where m is the weighted mean diameter of the bed in mm.

The scour depth is some multiple of D /15/. Equation 4.10 is developed by Valentin /47/:

$$\log(\frac{y_K}{y_1}) = \frac{F_{r1} - 2.0}{4 \cdot 7} - 0.55 \log(\frac{d_{90}}{y_1}) \quad (4.10)$$

where,

y_K = maximum scour depth

y_1 = depth of jet

F_{r1} = Froude number of incoming jet

d_{90} = most influential diameter of grain where 90 % by weight of the material is finer.

Equation 4.11 is developed by Altinbilek and Basmaci /4/:

$$\frac{S_T}{b} = (\frac{\tan\phi}{D_g/b})^{1/2} \times (\frac{F_r}{\sqrt{s-1}})^{3/2} \quad (4.11)$$

where,

S_T = terminal scour depth ,

b = the characteristic lenght of the obstruction along which sediment pick-up occurs,

ϕ = angle of repose of bed material,

D_g = the geometric mean diameter of the sediment particles ,

F_r = Froude number ,

S = specific weight ratio of bed material.

Equation 4.3 (sec. 4.2.3.1) developed by Catakli et al:

$$t_m + h_2 = K\frac{q^{0.6}(H_o+h)^{0.2}}{(d_{0.90})^{0.1}} \quad (4.3)$$

Equation 4.8 (sec. 4.2.3.2) developed by Zimmermann is

$$\frac{h_2 + t_K}{\left(\frac{h_2}{q^{2/3}}\right)^{0.73}} = 2.23 \frac{q^{0.72}}{(d_{85})^{0.08}} \quad (4.8)$$

Equation 4.12 is developed by Schoklitsch /52/ (cited in ref /40/):

$$d_s = \frac{3.15}{d_{10}^{0.32}} H^{0.2} q^{0.57} \qquad (4.12)$$

where,

d_s = the maximum depth of scour below tailwater level,

H = the total head from the headwater level to the tailwater level,

g = the unit discharge of the spill water,

d_{10} = the diameter of the bed material in mm with only 10 % coarser.

In the above mentioned equations it can be clearly seen that the maximum depth of scour is inversely proportional to the $1/n^{th}$ root of the diameter of bed material particle. The maximum scour depth decreases when the grain size of the bed material increases. However, some researchers in India have argued that the depth of scour downstream of rigid structures is unaffected by bed material being dominantly due to flow pattern. Another researcher called Veronese made a further study of the Schoklitsch equation, eqn. 4.13, and showed that the effect of the size of material was minor and he modified equation 4.12 as

$$d_s = 1.90 H^{0.225} q^{0.54} \quad (m) \; /52/ \qquad (4.13)$$

Analyzing the relationship between settling velocity and diameter of particles, i.e.,

- for weighted mean diameter m upto 0.10 to 0.12 mm, settling velocity $\propto$ (diam)^2
- for m upto 0.5 mm, settling velocity $\propto$ (diam)
- for m 0.5 mm, settling velocity $\propto \sqrt{diam}$,

Framji deduced that depth of scour must depend little on
diameter if tis grade exceeds 0.5 mm, the effect due to
viscosity becoming negligible /15/.

From the equations 4.9 to 4.12, from the above deduction of
Framji, and from the reasoning in sec. 4.2.1, eqs. 4.1 and
4.2, the effect of a larger grain size is to produce a
smaller scour depth. Model invesitgation should be made
to find the relationship between the maximum scour depth
and grain size for every individual case since a general
formula is not available. the degree of influence of bed
material can be estimated with model tests.

4.3.2 Effect of Apron Length

Ahmad /2/, and Fanti and Zbikowski /13/ studied the effect
of apron length on maximum scour depht. Fanti and Zbikowski
have formulated the following relationship between maximum
scour depth and apron length, Froude number and time:

$$h = h_n e^{-ba_1 F_r} t^{a_1} \qquad (4.14)$$

where,

h = maximum scour depth, m

a_1 = 0,17 + 0.00095 L,

L = apron length,

F_r = Froude number,

t = time after which the maximum scour depth
is measured, hrs,

h_n, b = coefficients, they generally depend on the
shape and construction of the spillway,
the bed material characteristics, and on
the degree of jump submergence,

e = the base of natural logarithm.

Ahmad has shown his results, graphically (see fig. 4-11).

From equation 4.14 and figure 4-11 it can be seen that
increase of apron length results in decreasing of scour
depth. the ratio of the lower depth after the longer apron
to the larger one after the shorter apron increases with
duration of scour. That means that the effect of apron
lengthening decreases with time. The effect of apron
lengthening is the greater the shorter is the apron to
be lengthened. If the apron is long, its lengthening is
ineffective /13/.

Since the effect of apron lengthening decreases with time,
as mentioned in the above paragraph, comparison between the
effects of different lengths should be made when the
scouring process approaches the equilibrium state. By
using sufficiently long solid apron the maximum depth of
a scour hole can be obtained within the limit required
by safety. However, one has always to bear in mind the
economy aspect so that an optimum design can be produced.
The study of the effect of apron length on maximum scour
depth helps to decide on the extent of the prevention or
protection work to be constructed to withstand the local
scour or if the scour can be allowed without any serious
damage to the structure.

4.3.3 Effect of Appurtenance Structures

4.3.3.1 End Sills

An investigator called Minor has tested the effect, on
scour depth, of three different types of sills, namely,
rectangular step, inclined teeth, and inclined plane
which are shown in figure 4-19, below /3/:

SHAPE 1   SHAPE 2   SHAPE 3
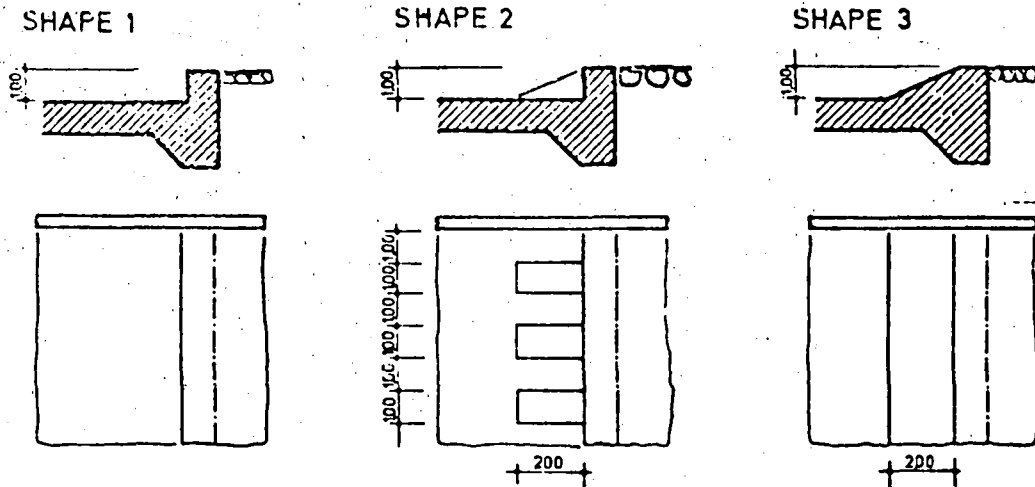
Figure 4-19. Different shapes of the end sill./30/

The results he obtained show that the scour depth for
shape 3 is lesser than for shape 2 and that for shape
2 is lesser that for shape 1. This can be observed from
the graphical representation in figure 4-20. The larger
depth of scour for shape 1 can be attributed to the
disturbance of flow due to the sudden transition when
compared to shape 2 and shape 3. Higher disturbance creates
strong turbulence which is responsible for deeper scour.
Shape 1 and shape 2 have relatively smoother transitions
and can have the effect of throwing the high velocity flow
toward the surface, thereby, ensuring lesser scour and,
hence, lesser depth of scour hole.

shape 1 of end sill
shape 2 of end sill
shape 3 of end sill
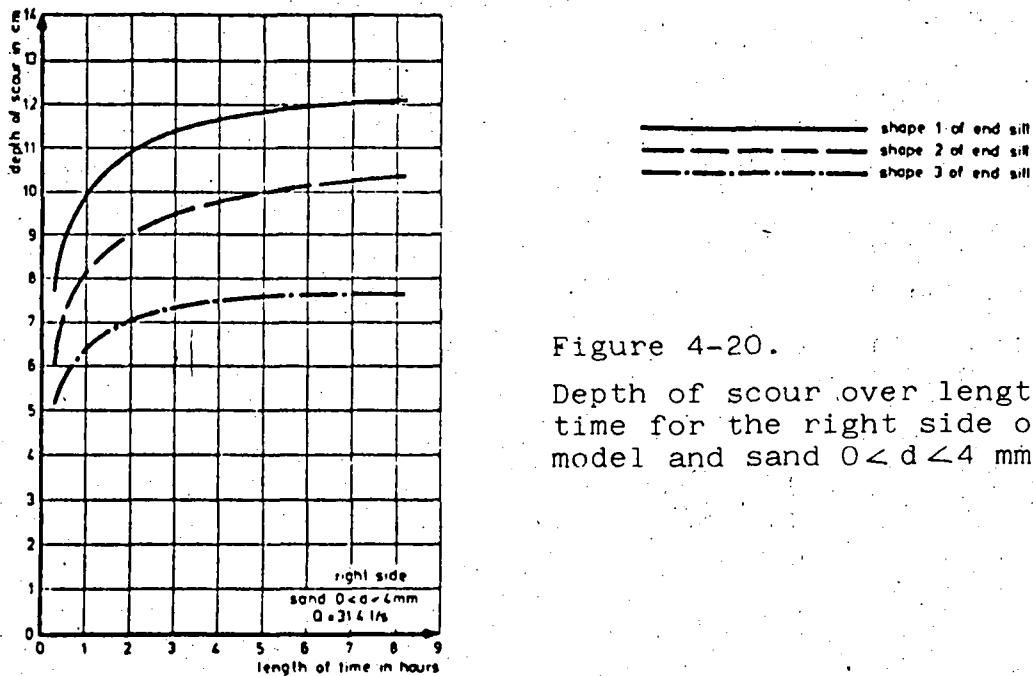
Figure 4-20.

Depth of scour over length of
time for the right side of the
model and sand $0 < d < 4$ mm./30/

Reconsidering the experimental model test results by ⌐atakli which was discussed in sec. 4.2.3.1, the effect of end sills on scour depth can be analyzed from equation 4.3.

$$t_m + h_2 = K \frac{q^{0.6}(H_o+h)^{0.2}}{d_{0.90}^{0.10}} \qquad (4.3)$$

K values (see sec. 4.2.3.1):

    for stilling basins without sill = 1.614
    for stilling basins with 2/4/6 sill = 1.531.

Thus, if all other parameters are kept constant the effect of end sills is to decrease the scour depth, t_m. The degree of decrease with different trapezoidal end sills is not the same as with the trapezoidal end sill 2/4/6. The K-values for two other trapezoidal end sills are given in ref /9/ and the procedure developed to obtain these values is stated in the above reference.

From the test results of Catakli et al, and Minor, it can be summerized that provision of end sills results in smaller scour depths and different end sills have different degrees of influence on the scour depth. The best shape of end sill for individual cases should be selected through investigation.

4.3.3.2 Baffle Piers

The studies of Framji, and Zimmermann and Maniak dealing with the effect of baffle piers are briefly mentioned in sec. 4.2.3.2 in connection with the scour length as the main concern. The same studies can be analyzed to see the effect of baffle piers on the depth of scour.

In the case of scale model study of the scour in Kotri
barrage Framji obtained a depth of scour equal to 15.5 m
(= 51 ft) below tailwater level without using baffle piers.
When two pairs of staggered blocks (one pair just downstream
of the glacis and another at the end of the riged pavement)
were used, the scour depth was reduced to 12.5 m (= 41 ft)
below tailwater level./15/

In the study of Zimmermann and Maniak the depths of scour
holes with baffle piers and without baffle piers can be
estimated from equation 4.4 and equation 4.7, respectively.

$$l_K = 10.7 \, t_K \qquad\qquad (4.4\ a)$$

$$5t_K \le l_K \le 7t_K \qquad\qquad (4.7\ a)$$

The depth of scour with baffle piers is

$$t_K \approx \frac{l_K}{10.7} \qquad\qquad (4.4\ b)$$

and without baffle piers, considering the upper limit,
the scour depth is

$$\frac{l_K}{7} \le t_K \le \frac{l_K}{5} \qquad\qquad (4.7\ b)$$

Comparison of equations 4.4 and 4.7 shows that the depth
of scour with baffle piers is lesser than the depth of scour
without piers.

The outcome of the studies by the above investigators
indicates clearly that the depth of scour decreases with
the provision of baffle piers. Since different shapes of
baffle piers can have different degrees of influence as in
the different shapes of end sills, and since the arrangement
of the piers also matters very much /53/, a general formula

cannot be obtained to estimate the effect of different
baffle piers on the depth of scour. Estimations should be
made from model tests and empirical equations developed
under similar conditions.

4.3.3.3 Chute Blocks

The effect of chute blocks is to increase the scour size /43/.
Depth of scour hole being one of the dimensions of the scour
hole, it should be increasing along with the increase of
the size of scour hole. A possible explanation for the increase
of scour size when chute blocks are provided is given in
sec. 4.2.3.3.

4.3.4 Effect of Flow Characteristics

4.3.4.1 Discharge

Catakli et al /9/, Lacey /15/, and Ahmad /2/ have found
that the depth of scour below solid apron varies directly
with the discharge intensity per unit length raised to the
exponent $2/3^{rd}$ as shown in equations 4.3, 4.9 and 4.15,
respectively.

$$t_m + h_2 = K \frac{q^{0.6}(H_o+h)^{0.2}}{(d_{0.90})^{0.10}} \qquad (4.3)$$

$$D = 0.9 \left(\frac{q^,}{f}\right)^{1/3} \qquad (4.9)$$

$$\frac{R}{q^{2/3}} = \text{constant} \qquad (4.15)$$

In equation 4.15 R = maximum depth of scour,,

q = discharge intensity per unit length.

Zimmermann and Maniak obtained the dependence of scour depth on discharge to be as $q^{0.24}$ as can be seen in equation 4.8 /53/:

$$\frac{h_2 + t_K}{(h_2/q^{2/3})^{0.73}} = \frac{2.23\ q^{0.72}}{(d_{85})^{0.08}} \qquad (4.8)$$

An empirical equation, eq 4.16, established by Wu for predicting limiting scour depth for dams in Taiwan shows that scour depth depends directly with $q^{0.51}$.

$$\frac{d_s}{H} = 2.11\left|\frac{q}{(gH^3)^{1/2}}\right|^{0.51} \qquad (4.16)$$

where d_s, H, and q are as in equation 4.12.

The effect of discharge on scour depth was also studied by Minor and he has presented his result graphically as shown in figure 4-21.
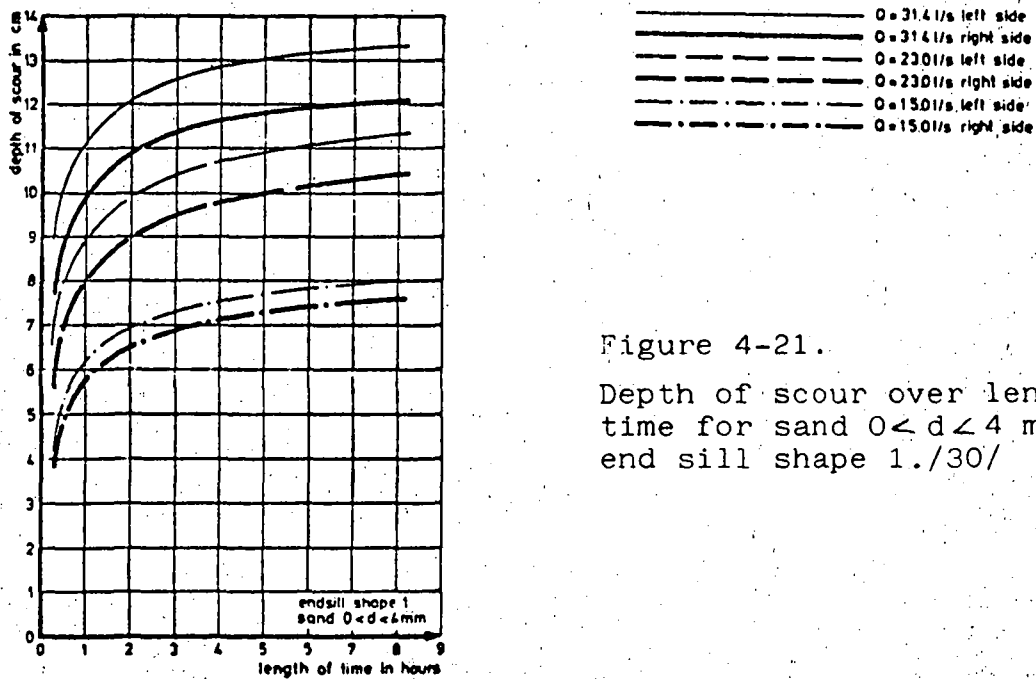
Figure 4-21.

Depth of scour over length of time for sand $0 < d < 4$ mm and end sill shape 1./30/

From the foregoing presentation, it can be observed that, in general the depth of scour increases along with the increase of discharge intensity. Except between the equations 4.3, 4.9, and 4.15, the degree of influence of discharge obtained from different tests is not identical. This may be because of different flow patterns occuring for different conditions of studies. To obtain the effect of discharge on scour with higher certainity, model tests should be carried out for every individual case.

4.3.4.2 Froude Number

Fanti and Zbikowski studied the relationship between Froude number and scour depth among other factors for flow passing over ogee crest through solid apron to erodible bed. The outcome of their study can be seen in equation 4.15:

$$h = h_n e^{-ba_1 F_r} t^{a_1} \qquad\qquad (4.14\ a)$$

$$ht^{-a_1} = h_n e^{-a_1 F_r} \qquad\qquad (4.14\ b)$$

Their experimental result plotted as ht^{-a_1} versus $a_1 F_r$ is given in figure 4-22 /13/. (See the results on two-dimensional model.)

According to the above investigators result, it can be clearly seen that scour depth decreases when the Froude number is increased.
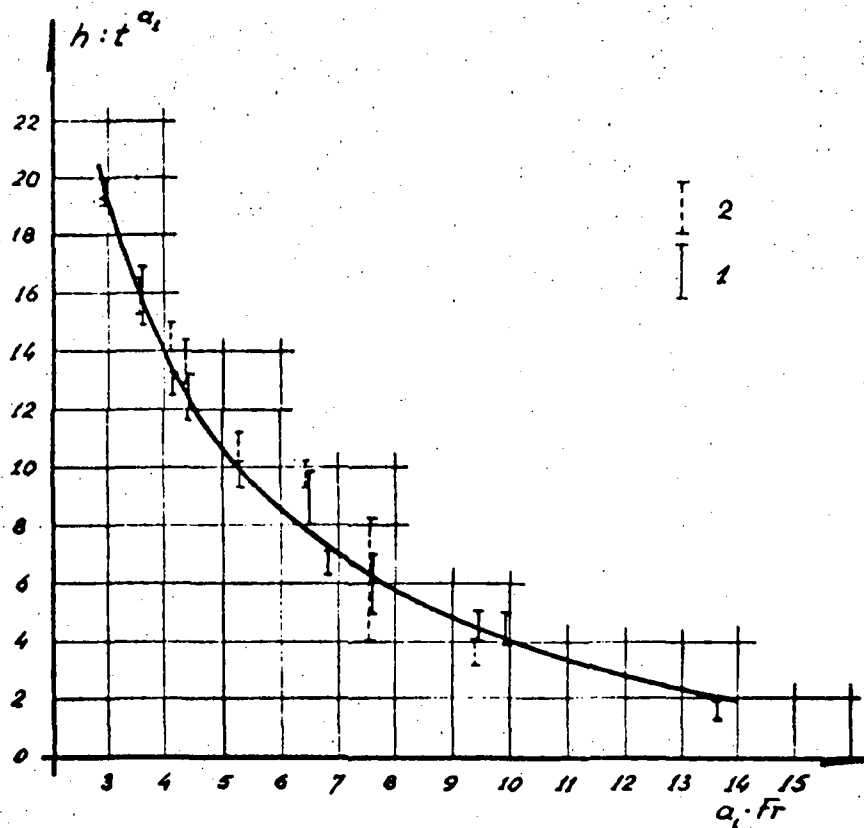
Figure 4-22./13/

Relationship $h \cdot t^{-a_t} = h_n \cdot e^{-b a_t Fr}$.

(1) The results on the two dimensional model;

(2) The results on the three dimensional model.

Valentin's study of scour in the case of flow under gates shows a result which contradicts the result by Fanti and Zbikowski. See equation 4.10 and figure 4-23./47/

$$\log\left(\frac{y_K}{y_1}\right) = \frac{F_{r1} - 2.0}{4.7} - 0.55 \log\left(\frac{d_{90}}{y_1}\right) \quad (4.10a)$$

$$\frac{y_K}{y_1} \cdot \left(\frac{d_{90}}{y_1}\right)^{0.55} = \frac{F_{r1} - 2.0}{4.7} \quad (4.10b)$$
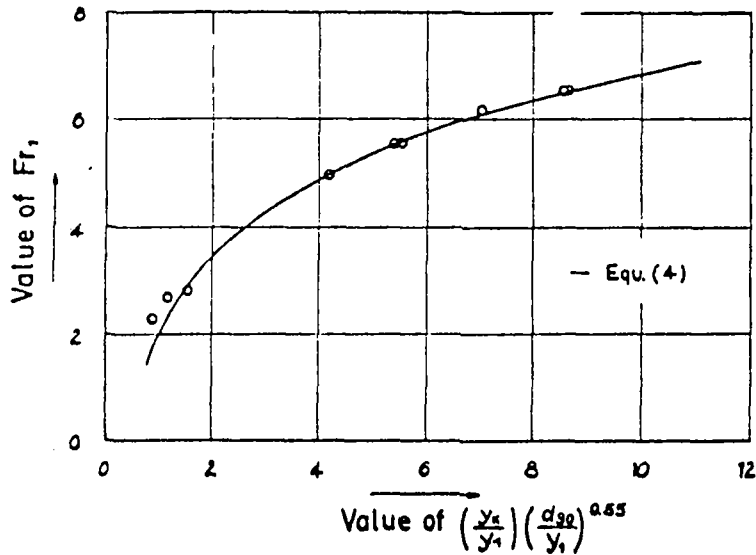
Figure 4-23.   Dimensionless scour depth.
Comparison between calculated
and experimental values.

Altinbilek and Basmaci have done a study which is closely
similar to that of Valentin and the relationship they have
obtained between ultimate maximum scour depth and Froude
number can be seen in equation 4.11:

$$\frac{S_T}{b} = (\frac{\tan \phi}{D_g/b})^{1/2} \cdot (\frac{F_r}{\sqrt{s-1}})^{3/2} \qquad (4.11)$$

This equation shows a relationship between Froude number
and depth of scour which also contradicts the one obtained
by Fanti and Zbikowski.

Increase of Froude number is associated with increase of
flow energy. Increase in energy of flow in the vicinity of
an erodible bed increases the local scour and, hence, growth
of scour depth is normally expected with the increasing of
Froude number. The model used by Fanti and Zbikowski is
provided with an end sill. The unfamiliar result they
obtained may be because of the ease with which the higher

velocity jet to be deflected by the end sill toward the surface of the flow which can result in lesser disturbance of erodible bed. However, to understand and explain the situation with certainity, careful observation of the model tests leading to contradicting results is required.

4.3.4.3 Tailwater Depth

From the empirical formula developed by Catakli et al, eqn. 4.3, it can be seen that the effect of increasing tailwater depth, E_d, is to decrease the maximum scour depth, t_m.

$$t_m + h_2 = K\frac{q^{0.6}(H_0+h)^{0.2}}{(d_{0.90})^{0.10}} \qquad (4.3)$$

Fanti and Zbikowski studied the effect of jump submergence on scour depth. According to these researchers, the increase in the degree of submergence upto some value of ratio E_d/E_1, where E_d = tailwater depth, and E_1 = depth of flow upstream of weir, caused the decrease of the scour depth. The minimum scour depths occured when the values of ratios E_d/E_1 changed in the limits 0.67 - 0.75, see figure 4-24.
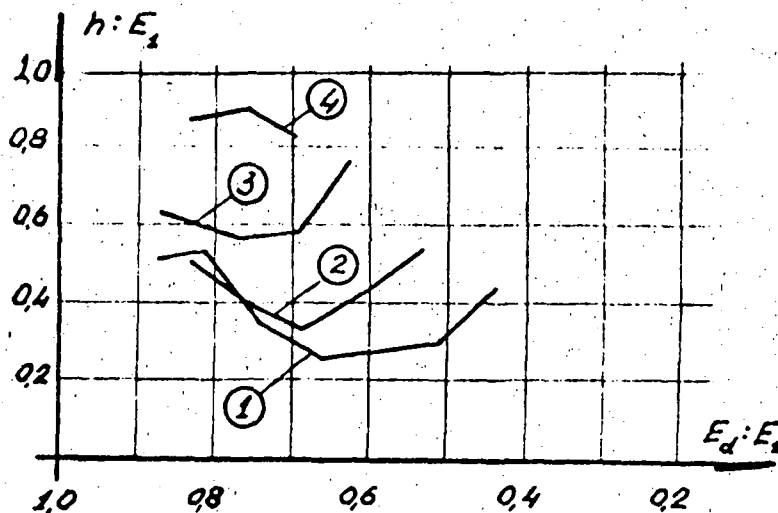
Figure 4-24. /13/

Relationship : $h : E_1 = f/E_d : E_1$.

(1) $F_r = 30.$
(2) $F_r = 20.$
(3) $F_r = 12.$
(4) $F_r = 9.$

For greater and smaller values of E_d/E_1 the scour depths increased. Generally the influence of submergence on the scour was negligible./13/

The increase in scour depth for lower and higher values of E_d/E_1, outside the limits 0.67 - 0.75, may be explained as follows: For lower tailwater depths the perfect jump may not be formed and for higher tailwater depths the jump may be drownd, and if it happens so energy dissipation reduces in both cases. The lesser the dissipation of the flow energy the higher will be the scouring capacity of the flow. This will result in the increase of the depth of scour hole. To check if the above explanation holds true or not, a close observation of the flow characteristics, for the specified conditions, is necessary.

4.3.4.4 Prediction

Studies have been carried out by many investigators and researchers to find relationships existing between instantaneous depth of scour hole   and duration of scour and between ultimate dimensions of scour and the factors involved in the development of scour with the intent of establishing a general rule which can be applicable for a wide range of conditions. As a result, various empirical equations are established, some of which are mentioned in the foregoing sections of this chapter. Some others will be discussed in this section. Dimensional reasoning and experimental and field data, taking the significant factors into consideration, have been used in the development of the equations.

Among many investigators and researchers Breusers, Watkins, Mehrotra, and Fanti and Zbikowski studied the variation with time of scour depth after solid protective apron.

Breusers formulated the following relationship:

$$\frac{h_{max}}{h_o} = (\frac{t}{t_1})^{\alpha} \qquad /7/8/ \qquad (4.17a)$$

where h_{max} =   maximum depth of scour,

h_o =   water depth at the end of bottom,
protection ,

t =   time ,

t_1 =   t at which $h_{max} = h_o$,

α =   exponent.

Plotting h_{max}/h_o versus t/t_1 from his experimental data on a log-log paper, he found that the plotted points were on a straight line. From his experimental results he obtained the value of exponent $\alpha = 0.38$. Thus,

$$\frac{h_{max}}{h_o} = (\frac{t}{t_1})^{0.38} \qquad /8/ \qquad (4.17b)$$

Watkins followed basically the same procedure as Breusers and plotted logD versus log t, where D = maximum depth and t = time. However, the plotted points did not lie on a straight line. Continuing his study further, he expressed the variation of scour depth with time by the equations

$$t - t_o = C \left[e^{mD} - e^{mD_o} \right] \qquad (4.18a)$$

or, $$t - t_o = C \left[10^{mD} - 10^{mD_o} \right] \qquad (4.18b)$$

where,

t =   time,

t_o =   time corresponding to D_o,

D =   maximum depth ordinate of scour profile,

D_o =   the nominal value of D = 0,

C =   time factor.

He has reported that his experimental data and the data by
Breusers fit the above equations very well. The points of
D versus log $(t-t_o)$ plot as a straight line except near
the origin./50/

Mehrotra also plotted maximum depth of scour versus time
and found a very similar result to that of Watkins /29/.
On the other hand, Fanti and Zbikowski established an
equation, eqn. 4.14, relating scour depth with time among
other factors, which has some similarity with eq. 4.17 by
Breusers /13/.

It is very difficult to say which one of the foresaid
results is a reliable approach to predict the magnitude of
maximum scour depth at some time after the start of the
scouring process or at an equilibrium state. However, an
important thing which should be remarked here is that in
both approaches a straight line plot is obtainable. This
is important because the straight line can be extrapolated
to obtain scour depths beyond the duration of data collection.

Other investigators, such as, Altinbilek and Basmaci /4/,
Valentin /47/, Zimmermann /53/, and Catakli et al /9/ have
established relationships between ultimate maximum scour
depth and factors other than time see eqs 4.11, 4.10, 4.8
and 4.3. Each of these equations has to be used to predict
the scour in situations where conditions are similar to
those which occured when the equation is derived.

The most commonly used method of predicting scour hole
dimensions is scale model studies. The concepts of geometric
and hydrodynamic similarities are incorporated in the
construction , running, of the scale model, and in the
interpretation of the results of the model test. The
reliability of prediction using scale models depends on
how exactly the flow characteristics and the bed material
of the prototype are reproduced on a geometrically similar
model. Scale models are treated separately in chapter 5.

5. SCALE MODELS FOR LOCAL SCOUR

5.1 Basic Similarity Criteria

The flow prevailing below solid aprons of stilling basins, in the case of prototype structures, is fully developed turbulent flow. Similar type of flow has to be reproduced on the model so that the local scour in the prototype and its model will be closely similar and prediction of scour hole dimensions will be more reliable.

Under conditions of fully developed turbulent flow on the model, the Froude law ensures the similarity of water levels, and of structures of the velocity field, and the dynamic effect of the latter on the moveable bed. The Reynolds number has no influence under such condition of flow. The well known Froude law is expressed by

$$F_r = \frac{V}{\sqrt{gh}} \qquad (5.1)$$

where F_r = the Froude number ,
        V = mean velocity of flow ,
        h = depth of flow ,
        g = gravitational constant.

To ensure similarity,

$$(F_r)_{MODEL} = (F_r)_{PROTOTYPE}$$

or, the scale of Froude numbers, $(F_r)_r = 1$. Therefore, the scale of velocities becomes:

$$V_r = h_r^{1/2} \qquad (5.2)$$

where h_r = scale of depths.

The reduction of the model velocity according to the Froude
law will, when the model scale becomes sufficiently small,
necessarily mean reduction of the Reynolds number effects
can no longer be disregarded. When this condition is attained,
the model cannot be expected to show any conformity to the
prototype. The role of Reynolds number in determining the
applicability of the results obtained under the Froude law
is termed as the scale effect.

To asses whether the model fulfils that the flow is
independent of the Reynolds number, the following inequality
obtained from experimental results and Shields diagram has
to be satisfied /31/:

$$R_{e_*} = \frac{dV_*}{\mathcal{V}} > 3.5 \qquad (5-2)$$

where

R_{e*} = shear Reynolds number ,
d = grain diameter,
V_* = shear velocity,
    $= \sqrt{gsR} = \sqrt{(\mathcal{T}_o/\mathcal{P})} = V/\sqrt{(\lambda/8)}$,
$\mathcal{V}$ = coefficient of kinematic viscosity,
s = slope ,
R = hydraulic radius ,
$\mathcal{T}_o$ = wall shear stress ,
$\mathcal{P}$ = pressure ,
v = mean velocity,
λ = coefficient of friction head loss.

For complete absence of viscous effects, $R_{e*} > 400$. The
limiting condition, $R_{e*} > 3.5$, is important in particular
for the smallest grains in the mixture and the smallest
discharge on the model still causing sediment movement./31/

5.2 Model Scale Selection

Experiments must be carried out on undistorted models of
the structure and the downstream reservoir /31/, which means,

$$l_r = b_r = z_r \qquad (5.3)$$

where l_r = scale of lengths,
          b_r = scale of widths,
          z_r = scale of heights.

The bed material must have the same shape of the grain
distribution curve and the same compactness and natural
slope on the model as in the prototype./31/

For a model scale l_r the following equations give the scales
of sediment size d, its specific weight under the water
γ'_s, and of the specific sediment discharge expressed in
weight under water g'_s./31/

$$d_r (\gamma'_s)_r = l_r \qquad (5.4)$$

$$(g'_s)_r = (l_r)^{3/2} \qquad (5.5)$$

The lower limit of permissible reduction of sediment on the
model is about 0.5 mm /42/. If this cannot be kept for model
specific gravity = 2.65, i.e., for $(\gamma'_s)_r = 1$, a lighter
material should be chosen for the model.

The distorision of the relative roughness of the bed for
a short section of the channel downstream of the stilling
basin has practically no influence on the development and
size of the scour./31/

High flood peaks of short duration passing across hydraulic
structures is a frequent occurence in many places. The local
scour downstream of the structures is dependent on the length
of time for which the high flows persisted so that for
model investigations of the depth of scour hole a reliable
method for establishing the model/prototype time scale, t_r,
is required. For the definition of time scale which is
constant during the process, conformity of the scour hole
in the model and prototype is necessary /8/. The relative
depth of scour hole can be expressed as

$$\frac{h(x,t)}{h_o} = f(\frac{t}{t_1}, \frac{x}{h_o}) \quad /8/ \qquad (5.6)$$

where
$$\begin{aligned}
h_{(x,t)} &= \text{scour hole depth}, \\
h_o &= \text{water depth at the end of bottom} \\
&\quad \text{protection}, \\
x &= \text{distance from the end of bottom protection}, \\
t &= \text{time}, \\
t_1 &= \text{a characteristic time of the scouring} \\
&\quad \text{process}.
\end{aligned}$$

If the function f is the same in model and prototype, then
the time scale can be defined as the ratio of the t_1-values
/7, 8/.

Breusers /7 /8 / used an approach based on specific relation-
ship between the Einstein grain mobility parameter, ψ, bed
load parameter, ϕ, and the continuity equation per unit
width for the bed load scouring process in the scour hole
to determine the time scale relationship for two dimensional
scour adjacent to protective aprons in estuary closure
structures. His result is the scale relationship

$$n_t = (n_{ho})^{2.05} \times (n_\Delta)^{1.6} \times (n_{u_{max} - u_{crit}})^{-4}$$

$$(5.7)$$

where   n   represents scale: for example n_t = time scale,

$$\Delta = \frac{\rho_s - \rho}{\rho} ,$$

ρ_s = density of particles,

ρ = fluid density,

u_{max} = $(1+3r)\bar{u}$,

r = mean relative turbulence intensity,

$\bar{u}$ = mean velocity of flow,

u_{crit}= the critical mean velocity computed from the critical shear velocity as given by Shields.

Farhoudi and Kenneth /14/ have extended Breusers research to the case of local scour downstream a hydraulic jump. Their work will be briefly described in the following paragraphs.

The continuity equation per unit width for the bed load scouring process in the scour hole can be expressed as

$$\frac{\partial y}{\partial t} = \frac{\partial q_B}{\partial x} = 0 \qquad\qquad (5.8)$$

where q_B = the bed load transport in volume per unit time,

t = time,

x,y = the coordinates of a point on the bed of a scour hole with origin at the end of solid apron.

Time scale of local scour resulting form eq.(5.8) can be written as

$$(t)_r = (q_B)^{-1} (y)_r (x)_r \qquad\qquad (5.9)$$

But $(x)_r = (y)_r$, since the scour tests are carried out on undistorted model (see sec. 5.2), and eq.(5.9) becomes

$$(t)_r = (q_B)_r^{-1} (L)_r^2 \qquad\qquad (5.10)$$

where   L = a characteristic linear dimension.

Farhoudi and Kenneth adopted the following correlation between ϕ and ψ:

$$\phi \;=\; 40(\psi^{-1/2} - \psi_{crit}^{-1/2})^3 \qquad (5.11)$$

By using equation 2.10b into equation 5.11 and combining the resulting equation with equation 2.11 an expression for q_B can be obtained. Finally using the expression for q_B in equation 5.10 gives a relationship for time scale,

$$(t)_r \;=\; (S_s-1)_r \; (V_* - V_{crit})^{-3}(L)_r^{-2} \qquad (5.12)$$

Channel velocity, V, is related to shear velocity by the expression

$$V \;=\; 2.5V_* \; \ln(\frac{12.3\ d}{})\qquad (5.13)$$

where d = depth of flow
              = effective bed roughness.

Since the logarithm term does not change very much because the model bed material is seldom larger than in the prototype, equation 5.12 can be written as

$$(t)_r \;=\; (S_s-1)_r \; (V_{max}-\bar{V}_{crit})^{-3} \; (L)_r^2 \qquad (5.14)$$

V_{max} and $\bar{V}_{crit}$ are the same as u_{max} and u_{crit}, respectively, in equation 5.7.

The value of the index for (S_s-1) obtained by experiment is 1.4. Thus, the time scale relationship becomes

$$(t)_r \;=\; (S_s-1)_r^{1.4}(V_{max} - \bar{V}_{crit})^{-3}(L)_r^2 \qquad (5.15)$$

Farhoudi and Kenneth have laso presented, in their report, an example to demonstrate the calculation of time scale using equation 5.15.

6. MEASURES TO AVOID LOCAL SCOUR

6.1 Prevention

The kinetic energy at the base of a hydraulic structure
must be dissipated in order to prevent the possibility of
severe scouring of the downstream river bed and the
undermining of the foundation which endangers the dam safety.
Hydraulic energy dissipators are needed for this purpose.

Operation of any hydraulic-energy dissipator depends largely
on expending part of the energy in high-velocity flow by
some combination: external friction between the waters and
the channel, or between water and air; or by internal friction
and turbulence. Fundamentally, energy dissipators or stilling
basins which perform the energy reduction, convert kinetic
energy into turbulence and finally into heat. Dissipation
of energy in the stilling basin is primarily accomplished
by means of a hydraulic jump.

6.1.1 Hydraulic Jump Basins

A hydraulic jump stilling basin reduces the exit supercritical
flow from the spillway to a tranquil state by a jump which
quickly dissipates flow energy through large-scale turbulence
such that the flow becomes incapable of scouring the down-
stream channel. To ensure that a stilling basin serves its
function effectively, it is important to design the basin
with the objective that for the range of design discharges
the elevation of the tailwater depths in the downstream
channel should be greater than or equal to the elevation
of the conjugate depths to prevent sweep out of the jump
from the basin. Conversely, if the conjugate depth is too
low, the jump will be drowned, loosing its purpose as an
energy dissipator.

A perfect hydraulic jump is formed when the elevation of the conjugate depth after the jump corresponds to the elevation of the tailwater depth. The floor elevation and width of stilling basins are selected such that the conjugate depth elevation must nearly agree with the tailwater depth elevations for a design discharge or for a range of discharges.

Stilling basins usually are not designed to confine the entire length of the jump because of the expenses. Certain accessory devices such as baffle piers, end sills, and chute blocks are installed along the basin floor to control and stabilize the jump and increase the turbulence which assists the energy dissipation. Their presence permits the shortening of the basin as well as providing a safety factor against the jump being swept out. Researchers have found out that the presence of the appurtenances of stilling basins reduces the tailwater depths required (sec. 6.1.1.2).

6.1.1.1 Design

The U.S. Bureau of Reclamation recommends the following stilling basin designs in relation to Froude numbers of the incoming jets into the stilling basin /46/:

a) Basins for $F_{r1} < 1.7$:

$$F_{r1} = \frac{V_1}{\sqrt{g d_1}}$$

$$V_2 = \frac{1}{2} V_1$$

$$d_2 = 2d_1, \text{ or } d_2 = 1.4 \, d_c$$

where F_{r1}, V_1, d_1 = Froude number, velocity and depth of flow before jump,

d_2 = depth of flow after jump,

d_c = critical depth (depth when $F_{r1} = 1$)

No special stilling basin is required for the above condition. Channel length beyond the point where the depth starts to change should not be less than about $4 \, d_2$.

b) Basins for $F_{r1} = 1.7 - 2.5$

There is no active turbulence in this range of Froude numbers. It is known as a pre-jump stage.

Baffles or sills are not required. Conjugate depths and basin lengths shown in fig. A1 (appendix) will provide acceptable basins.

c) Basins for $F_{r1} = 2.5 - 4.5$

True hydraulic jump does not fully develop. There is a wave action which cannot be controlled by the usual basin devices.

U.S. Bureau of Reclamation (USBR) basin type I shown in fig. A2 (appendix) is relatively effective for dissipating the bulk of the energy of flow. Because of the tendency of flow to sweep out and as an aid in suppressing wave action, the water depth in the basin should be about 10 % > d_2. The need for utilizing this type of basin in design can be avoided by selecting stilling basin dimensions which will provide flow conditions which will fall outside the range of transition flow.

d)   Basins for $F_{r1} > 4.5$

True hydraulic jump develops. Elements of the jump vary according to the value of the Froude number, F_{r1}.

For flow velocities $V_1 < 15$ m/s (= 50 ft/sec), USBR basin type II shown in fig. A3 (appendix) can be adopted. For flow velocities $V_1 > 15$ m/s USBR basin type III shown in fig. A4 (appendix) can be adopted. In the latter basin energy dissipation is accomplished primarily by hydraulic jump. It provides a longer basin than type II. The water depth in the basin should be about 1.05 d_2.

The generalized design usually results in safe stilling basins having a conservative safety factor. However, optimal determination of the floor elevation and basin width for minimum cost designs seldom have been achieved. Tung and Mays have developed an optimization model /45/ to determine the optimal floor elevation and basin width and corresponding dimensions of appurtenances of stilling basins for overflow spillways. The criterion used in selecting the optimal values of the decision variables, i.e. width and elevation of the stilling basin, is the minimization of the total construction cost of the stilling basin subject to the constraints: conservation of energy and momentum must be satisfied; performance of the stilling basin must be satisfied for a range of possible discharges; basin width cannot be narrower than the length of the spillway crest. Discussion of the optimization methodology is out of the scope of this paper.

For the case of a weir with a stilling basin with two rows of baffle piers, design formulas are developed by Zimmermann and Maniak with regard to a minimum scour /53/. The top view of the baffle piers is a square and its edge length a

was found in between:

$$0.5 \ t_{gr} \leq a \leq 0.7 \ t_{gr},$$

where $\qquad t_{gr} = \dfrac{q^{2/3}}{g^{1/3}}$

in which $\quad q$ = discharge per unit width, $m^3/s \ m$

$\qquad\qquad g$ = 9.81 m/s^2

Different arrangements of the baffle piers are shown in fig. 4-15. An arrangment of baffle piers according to type 4 in fig. 4-15 showed a reduced scour length.

6.1.1.2 Appurtenance of Stilling Basins

a.) End Sills

End sills perform the following functions:

- Push up the hydraulic jump towards the foot of the spillway or outlet structure. In the case of lower tailwater depth than the conjugate depth, the provision of end sills helps to raise the water level to that required for jump formation and prevent the sweep out of the hydraulic jump, i.e., end sills fascilitate the jump formation and also control the length of the jump. This will require a shorter solid apron which means less expensive construction./10/46/

- Prevent the scouring of the erodible bed immediately after the end of the solid apron End sills deflect the high velocity flow on an apron away from the river bottom toward the surface where it would be harmless. The upward deflection of the stream if not to sharp, creates a ground roller beneath it that tends to move any loose material on the river bottom

upstream toward the dam and deposit it at the end of
the apron. It is found that if the stream is deflected
upward too sharply with a sill with too steep an
upstream face, formation of the ground roller is
hindered./6/22/23/

- Improve the velocity distribution across the flow.
  This results in the formation of uniform scour profile
  through out the width of the channel and local scour
  can be treated as a two-dimensional problem.

- The particular feature of dentated end sills is that
  they break the continuity and compactness of the
  incident nape over a stilling basin so that
  concentration of flow will be reduced and some energy
  is also dissipated. The flow is fractioned in jets
  by the dentated end sills. The water passing over
  the dentals is thrown parabollically and returned by
  the water mass created by the natural river depth.
  The water passing through the separating channels
  between the dentals is thrown with divergent patterns
  the different jets striking each other./16/

Different shapes of end sills have different effects on
locals scour. The suitable shape for individual cases is
determined by model tests./9/30/

b) Baffle Piers

Their function is to dissipate energy mostly by impact
action. They are very useful in small structures with
low incoming velocities /10/.They are unsuitable, however,
where high velocities make cavitation possible. Blench
    et al have found that velocity distribution can be
imporved by two rows of staggered blocks /6/. According
to the above investigators the upstream set of baffle
piers (impact blocks) throws the line of maximum velocity

upwards, while the downstream set (deflector blocks) further improves the velocity distribution and creates a bed roller that deposits mobile material against the toe wall.

Baffle piers are not effective to push up the hydraulic jump. They cause only hurdling action. Staggered blocks in combination with a baffle wall are effective in pushing up the hydraulic jump./1/

c) Chute Blocks

Their function is to furrow the incoming jet and lift a portion of it from the floor, producing a shorter length of jump than would be possible without them. These blocks tend to stabilize the jump and thus to improve its performance /10/. There is a definite reduction of velocity when chute blocks are used but the velocity distribution differs only very little. There is a marginal contribution in energy dissipation by these blocks/43/.

6.1.1.3 Air Entrainment

Air is entrained at any surface of discontinuity; in jets moving with a high velocity; in the wake of a pier (or at any obstruction projecting out of water)· by small surface waves; and at the point of separation near the boundary curvature. In the supercritical flow on the glacis of a weir, air adjacent to the fast moving sheet of water moves along with it and is drawn in at the position where the supercritical flow dives into the subcritical. The entrained air is carried down with the diving jet, but being lighter, tends to escape towards the surface again. Heavy foaming and appearance of minute air bubbles at the standing wave are the manifestation of this air entrainment phenomenon.

Entrained air has the following effects /21/:

a) A little reduction in velocity at the foot of the spill-
   way,

b) Bulk air concentration of 15 - 20 % can reduce scour
   downstream of the stilling basin by 5 - 10 % in simple
   basins. The effect is less pronounced the more complex
   the basin

c) It stabilizes the flow and causes the hydraulic jump to
   form closer to the foot of the spillway.

Air can be entrained by establishing an air-water interface
on the underside of the nappe so that the flow of the water
draws the air into the stream without any assistance from
outside sources /21/. Another method is by constructing
aerodissipators. One type of aerodissipator is explained in
ref /19/.

6.1.2 Deflector Bucket

When the tailwater depth is too high or too low and jump
formation is not favourable deflector bucket can be used
as an alternative. This device is a large specially shaped
lip or bucket which throws the whole jet of flow into the
air. Part of the energy in the jet is dissipated in the air,
but in any case the jet falls back into the channel at a
safe distance from the dam.

With the origin of coordinates taken at the end of the lip,
the path of the trajectory is given by the equation:

$$y = x\tan\theta - \frac{x^2}{K\left[4(d+h_v)\cos^2\theta\right]} \qquad (6.1)$$

where, θ = the angle of the edge of the lip with the horizontal,

h_V = the velocity head of the flow,

d = the depth of the flow, and

K = a factor, equal to 1 for the theoretical jet.

In actual practice a value for K of about 0.9 should be assumed./46/

The horizontal range of the jet at the level of the lip is obtained by making y in equation (6-1) equal to zero. Then:

$$x = 4K(d+h_V) \tan\theta \cos^2\theta \qquad (6.2)$$
$$= 2K(d+h_V) \sin^2\theta$$

The angle of the lip is influenced by the bucket radius and the height of the lip above the bucket invert; ordinarily the exit angle is limited to no more than 30°./

6.2 Protection

In most cases, the flow after stilling basins will have a residual energy, the magnitude of which depends on the effectiveness of the stilling basin. The adverse effect of this residual flow energy has to be studied and estimated to decide, if protection for erodible bed below the solid apron is required or not. If some scour can be allowed without sacrificing the safety of the hydraulic structure, then, protection will not be required. If the situation requires the provision of protection, the length of protected region and the size of stable stones (or gravel) must be determined in such a way that economy and safety are optimized. However, in the following sections the above factors will be seen from the point of view of safety only, since information concerning economy could not be obtained at the moment.

6.2.1 Extent of Protection

The extent of protection should be limited to the channel
length that is most likely affected by local scour, when
the design discharge is released. The approximate estimate
of this length can be obtained by scale model analysis since
there is an approximate similarity between scour profiles
(sec. 4.1). It can also be estimated by empirical relations
based on model tests of individual cases, see eq. 4.2 in
sec. 4.2.3.1.

Determination of the transition zone below the hydraulic
jump is another possibility of knowing the length to be
protected. This can be done by measuring the maximum
instantaneous near bottom velocities, see fig. 4-1, and/or
the macroturbulence intensities of the flow as shown in
fig. 4-6. The transition zone ends at the section of the
channel where the normal channel flow starts. Knowing the
length of the transition zone, one can obtain the length of
scour using an empirical equation relating the above and
transition length. Such an equation is developed by Rand.

$$L_e = 1.15 \, L_t \quad /34/ \qquad\qquad (6.3)$$

where L_e = length of scour,
          L_t = transition length.

The length of scour should be provided with protection as
this is exposed to danger.

6.2.2 Size of Stable Stones

The commonly used method of protection is by covering the
erodible bed with stones of various sizes. The size
distribution pattern follows the intensity of the scouring
force such that the bigger sizes will take care of the more
severe condition./30/

The protective layer must be selected such as to ensure its own stability and prevent the bed material beneath it from being washed away. Protection will be efficient if the layer is graded to comply with the following condition:

a) The stones that make up the upper layer should withstand to a sufficient degree, the action of drag forces.

b) The base material should not be capable of passing through the voids left between the components of the upper layers.

The Terzaghi-Vicksburg criterion can meet the second condition /37/:

$$\frac{D_{15}\text{filter}}{D_{85}\text{base}} < 5$$

$$4 < \frac{D_{15}\text{filter}}{D_{15}\text{base}} < 20$$

$$\frac{D_{50}\text{filter}}{D_{50}\text{base}} < 25$$

The symbols are interpreted as follows:
D_{15} is the sieve size through which 15 % (by weight) of the filter will pass, etc.

The second condition may be met by the following empirical equation developed by Kumin /17/:

$$d_H = \frac{(0.255 \, V_o)^{10/3}}{h^{2/3}} \tag{6.4}$$

where d_H = size of stable stone, cm

V_O = non-eroding velocity for a given soil and averaged across the depth of a moderate turbulent uniform flow, m/s

h   = water depth within the section under examination, m.

The value of V_O is obtained from the equation

$$\frac{V_O}{V} = 0.87 \ (1+M) \qquad\qquad (6.5)$$

where   M = $\dfrac{U'_{max}}{\overline{V}}$,

U'_{max} = maximum pulsation velocity equal to difference of $V_{max} - \overline{V}$,

V_{max} = maximum actual velocity,

$\overline{V}$ = averaged velocity assumed for the after-jump section to be equal to mean velocity,

V = non-eroding velocity averaged across the flow of equal depth as in V_O, but of higher turbulence.

Gunko also has established an empirical equation to determine the size of stable stones for the case of flow downstream of solid or dentated end sill and dissipator spreader, the dimensions of which are shown in ref./17/. The equation is

$$\frac{100 \ d_H}{h} = 25.25 - \sqrt{237 - (\frac{x}{h} + 9D - 26.5)^2} - 5.18D$$

$$(6-6)$$

where $\dfrac{x}{h}$ = relative distance from the constriction below the end sill, see fig. 6-1

D = h_2/h_1
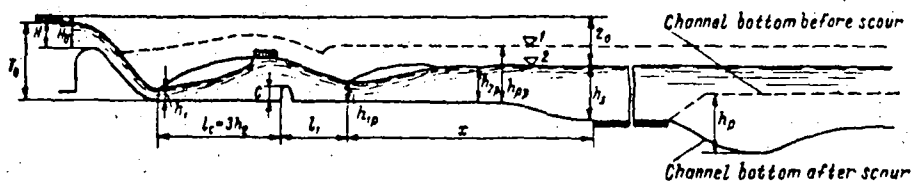
Figure 6-1. Definition sketch for spillway
             apron with end sill. /17/

The variation of values of D and x/h ranges /17/:

x/h	D
3.0 to 17.5	1.00
2.5 to 15.0	1.25
2.0 to 13.0	1.50

7.   MEASURING TECHNICS OF FLOW PARAMETERS

Some measuring technics of flow parameters which can be
applied in field investigation or laboratory study of flow
parameters are briefly presented in this chapter. In some
cases more than one alternative methods are given in which
case the investigator or researcher must choose the method
which best fits his purpose.

7.1   Bed Topography

First a grid, as shown in figure 7-1, has to be worked out
for the extent of region below the solid apron where scour is
expected to take place. At separate verticals in every
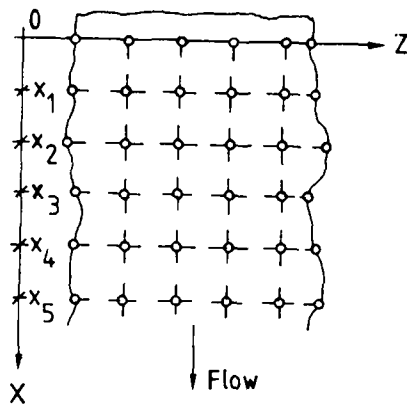
Figure 7-1.   A grid of bed topography
              measuring points.

section x_1, x_2,..., etc., the distance of which from the
x-axis are determined by measurement, the depth of the bed
is obtained. In large river channels the alignment can be
controlled by taking surveys (using a level or theodolite)
whereas in small streams a steel rope with longitudinal
divisions stretched across the river in the measuring
section is sufficient as reference. A steel rope can be
used also in laboratories.

In laboratory flumes, with at least one wall made of pyrex glass, pointed depth gage with sufficiently detailed divisions is used to measure the scour depths.

In field investigations of small streams the depth of the bed is measured by soundings taken from a boat. If the performance of a boat is affected by the disturbance of the flow, the sounding may be done from a cableway stretched across the channel. In the later case the cableway must be tightened properly so that it will not sag by the weight of the sounding equipment, otherwise the sag must be considered in the computation of the depth of the bed. For large river channels the depth is often measured by ultra-sonic depth gages, i.e., echosounders and echographs, based on the principle of reflection of ultrasonic waves from the bed. The error of echosounders is only a few centi-meters ./31/

Knowing the distances of the cross sections from the end of the solid apron and the measure of depths along each cross section, the profiles of the scour hole can be easily drawn. Contour lines of the scour hole can also be drawn for the entire scoured region.

7.2 Water Levels

The simplest way to measure water level is by means of a staff gage, a scale set so that a portion of it is immersed in the water at all times. The gage may consist of a single vertical scale attached to a rigid structure. If no suitable structure exists in a location which is accessible at all stages a sectional staff gage may be used. Short sections of staff are mounted on available structures or on specially constructed supports in such a way that one section is always accessible. An alternative to the sectional staff is an inclined staff gage which is placed on the slope of the channel and graduated so that the scale reads directly in vertical depth./27/

Water level change with time is done by recording the levels with stage recorders, the drums of which turn at a rate that can be altered accrding to the expected speed of oscillation of the water level and the aims of the measurements.

The vertical shafts of permanent recorders are built into the channel bank at the measuring section and are linked to it by a horizontal pipe sited beneath the lowest possible water level.

Temporaty transportable recorders are often used for measuring water levels (fig. 7-2). The float of the recorder moves in a vertical steel pipe closed at the lower end and with several small orifices symmetrically distributed over the circumference. The drum of the limnigraph is fitted at the top of the pipe, and a bench mark on the bank and an auxiliary mark on the vertical pipe of the limnigraph facilitate marking of the initial values of the height of the water level, together with time, before measurement on the recorder charts./31/
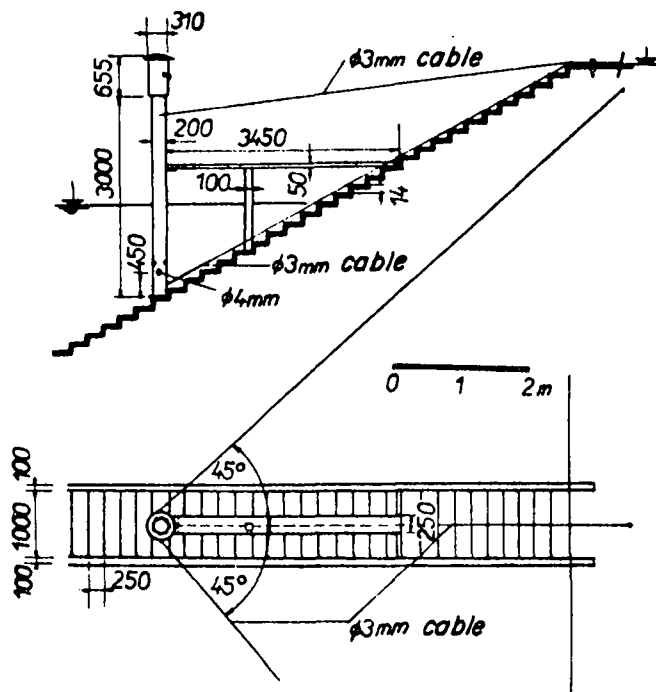
Figure 7-2. Temporary water level recorder./31/

Level recorders are very expensive and water level measure-
ment using staff gages must be prefered unless there is a
very great need foor continuous water level changes occuring
with the charge of time.

7.3 Velocities of Flow

The current meter is the most widely used instrument for
measuring the velocities of flow. It is reliable and
comparatively accurate when correctly used. It may have
different forms. The most common ones are propeller and cup
current meters. The purposes of a current meter are
indicating, recording and directional.

The propeller current meter is based on the principle that
the rate of its propeller revolutions is proportional to
the flow velocity at the point of measurement. After a
certain number of propeller revolutions an electric circuit
with a device for counting the revolution is closed.
During the metering period the average number of revolutions
per second is ascertained and from the calibration
certificate of the meter the value of the flow velocity
at the measuring point is determined. The meter is either
fixed to a rod or suspended. It is lowered into the flow
from a boat, a bridge or a cableway. With the aid of
current meters it is possible to measure the velocity at
separate points in the flow and in individual verticals,
or to investigate velocities in the whole section (isovels)
and also the mean cross-sectional velocity./27/31/

At every point the flow velocity is measured over a period
of time, which is long enough to exclude the influence of
flow fluctuations, but short enough to ensure that time
error in measurements are small and a certain steady state
of flow is recorded. For this reason several meters are
usually used simultaneously, either fixed to a mobile

perpendicular set of poles or to a horizontal frame of
measuring, a carriage, (in a rectangular section) moving in
a vertical direction (/31/, fig. 12-3)./31/

Point measurements with a current meter should last at
least one minute and during periodically recurring pulsa-
tions they should be at least as long as two periods. The
distance of the extreme measuring points from the water
surface, the bed and the sides, must not exceed 0.2 m and
maximum distance between the points can be 1 m, the spacing
of the measuring points near the bed and the channel sides,
where there is a great velocity gradient, should be smaller.
To obtain a sufficiently accurate picture of the velocity
field in a section during point measurements of velocity,
the number of measuring points x must lie within

$$24A^{1/3} < x < 36A^{1/3} \quad /31/ \quad\quad (7.1)$$

where
A = cross-sectional area of the measured
section, m^2.

Another device which is used to measure point velocity is
the Pitot tube. The principle of this device can be found
in many fluid mechanics or hydraulics books.

7.4 Discharge

The most frequently used method for measuring discharges on
rivers and canals consists of measuring the cross-sectional
area A (corresponding to the water stage h) and the
simultaneous measurement of the mean flow velocity, v,
with the aid of current meters. The steady discharge Q
corresponding to the stage h is then given by

$$Q = Av \quad\quad (7.2)$$

The number of velocity determinations must be limited to those which can be made within a reasonable time interval. This is especially true if the stage is changing rapidly, since it is desirable to complete the measurement with a minimum change in stage.

The practical procedure involves dividing the stream into a number of vertical sections (fig. 7-3). No section should include more than about 10 % of the total flow. On the basis of many field tests, the variation for most channels is such that the average of the velocities at 0.2 and 0.8 depth below the surface equals the mean velocity in the vertical. The velocity at 0.6 depth below the surface is also nearby equal to the mean in the vertical./27/
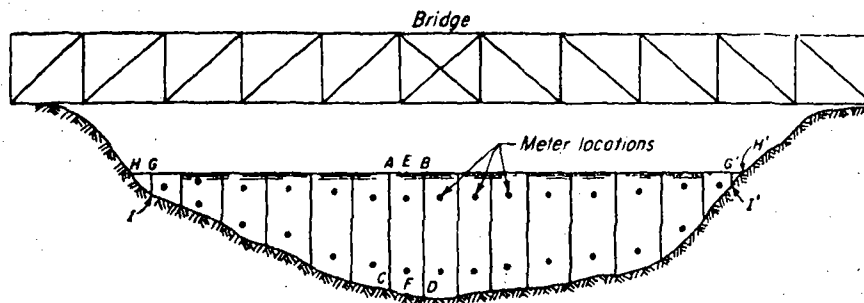
Figure 7-3. The procedure for current-meter measurement.

Computation of total discharge is made as follows:

a) Compute the average velocity in each vertical by averaging the velocities at 0.2 and 0.8 depths.

b) Multiply the average velocity in a vertical by the area of a vertical section extending halfway to adjacent verticals (ABCD, fig. 7-3). This area is taken as the measured depth at the vertical (EF) times the width of the section (AB).

c) Add the increments of dicharge in the several verticals. Incremental discharge in the shore section (GHI, fig. 7-3) is taken as zero./27/

If a number of similar measurements of discharge for
various steady stages h is carried out, a rating curve
expressed as

$$Q = f(h) \qquad (7.3)$$

can be established. From this discharge Q through the
section for any arbitrary water level h can be determined.
A necessary condition is that the section should be
situated in a river or canal reach unaffected by backwater
and should have a stable bed.

Another method of discharge measurement is the use of
temporary or permanent gauging structures. These structures
are usually broad crested notches or wiers which have
been developed on the basis of laboratory studies. The
discharge is calculated as a function of the head above
the crest of the spillway. Although the structures have
been investigated on models, in special circumstances
(effect of bends, sedimentation, etc.) it is advisable
to verify several discharges by direct measurements in the
field /31/.

On smaller canals and rivers it is also possible to use a
sharpe-edged notch or a Venturi or Parshal measuring flume
for discharge measurement. Even if the equations for the
calculation of the discharge on these devices are known
on the basis of measured geometric and hydraulic parameters,
in special circumstances their accuracy should again be
verified by calibration.

Other methods are also used for discharge measurement on
rivers and canals, e.g., dilution gaging. In this method
a known quantity of tracer (e.g. isotope) solution at known
concentration is injected into the stream with the aid
of special dosing equipment and at a downstream section,

after perfect mixing, its concentration in the water is
measured, e.g. with the aid of radiation counter. The
discharge is then calculated from the equation

$$Q = q \; \frac{C_1 - C_2}{C_2 - C_o} \tag{7.4}$$

where,

q = injection rate

C_o = background concentration

C_1 = tracer concentration at injection

C_2 = downstream sample concentration.

7.5   Sediment Measurement

Sediment transport takes place either along the bed (sand,
gravel, boulders) or in suspension (fine particles).

Coarser sediment transport along the bed is measured either
by direct mechanical methods or indirect methods.

Direct measurement for research purposes on small streams
consists of a grated opening (pit) in the stream bed into
which the bed material falls. The trapped material is
latter excavated or sluiced out and measured.

Direct measurement in larger rivers is achieved by the aid
of portable bed load meters lowered to the bed of the river.
Portable bed load meters consist of a container. The
pressure difference sampler /27/ and the VUV bed load meter
/31/ are among the samplers used for bed load measurement.

A good sampler must cause minimum disturbance of streamflow,
avoid errors from short period fluctuations in sediment
concentration, and give results which can be related to
velocity measurements.

The pressure difference type of bed load sampler is shown
in figure 7-4. The expansion section causes a pressure
drop which encourages inflow at the same rate as the
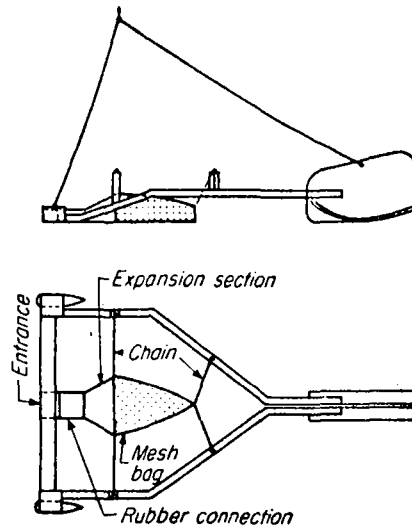
Figure 7-4.   Pressure-difference type of
               bed-load sampler as developed
               by the Netherlands government.

prevailing flow while at the same time the reduced exit
velocity encourages deposition of sediment in the mesh bag.
Fine sediment particles can escape through the mesh, and
a calibration in a flume is desirable./27/

Indirect methods include acoustic, electric and optical
methods, the use of radioactive and fluorescent tracers,
etc. The basic principles of these methods could not be
included due to lack of adequate information.

Suspended sediment concentration is measured either directly
by taking individual or pumped samples from the flow or
indirectly with the aid of turbidity meters based on the
principle of photoelectric effect. A number of commercially
produced meters exist for the measurement of suspended

sediments. The simplest instrument is a sampling bottle
with an inlet and de-aeration office, which is placed in
the stream until it is full.

Instead of point sampling it may also be used for integra-
tion sampling vertically. In this case the sampler is
lowered through the stream at constant vertical speed until
the bottom is reached and is then raised to the surface at
constant speed. The duration of the traverse is determined
by the time required to nearly fill the sample bottle and
can be computed from the filling rate curves for the
particular nozzle when the stream velocity is known./31/27/

8. CONCLUSION

1. Local scour is, principally, a bed load transport
    phenomenon. In the process of local scour the drag and
    lift forces destabilize the particles of the bed material
    while the submerged weight of the particles tends to
    stabilize them. For a particle to start motion, the
    shear stress acting on the particle must overcome the
    critical shear stress existing between the moving
    particles on the surface of the erodible bed and the
    bottom layer.

2. Scour activity increases with turbulence intensity.
    High turbulence intensity occuring at the point of
    reattachment of the main stream, at the downstream end
    of the region of flow separation, manifests peak local
    scour activity. This activity decreases with the
    increase of scour hole depth and goes on diminishing
    as the ultimate depth of scour is approached.

3. Clear-water scour is more severe than scour with
    sediment loaded water, and almost all investigators and
    researchers have been giving attention to the problem
    of clear-water scour. Scour hole develops faster and
    deeper in clear-water scour and the increase of the
    scour hole depth is asymptotic with time. Stable
    configuration of scour hole profile is reached in scour
    with sediment loaded water. The time to reach a stable
    configuration is the shorter, the higher is the sediment
    load.

4. An approximate similarity exists between pot-hole scour
    profiles of geometrically similar models for all ranges
    of discharge, duration of scour, and particle size above
    a limiting diameter of 0.5 mm. Under conditions of
    fully developed turbulent flow on a model, the Froude

law ensures the similarity of water levels and of the
structure of the velocity field and the dynamic effect
of the latter on the moveable bed. The condition for
fully developed turbulent flow is the shear Reynolds
number, $R_{e*} > 3.5$ for the smallest grains in the mixture
and the smallest discharge on the model still causing
sediment movement. For complete absence of viscous
effects $R_{e*} > 400$.

5. The length of scour hole:

   - increases with the decreas of particle size of the
     bed material ;
   - increases with the decrease of length of solid apron
     since decrease in solid apron length means increase
     of the unprotected region of the tranzition zone
     where scour activity prevails ;
   - increases with provision of end sills ;
   - decreases with the provision of baffle piers ; and
   - increases with the provision of chute blocks.

   Model study should be carried out to obtain a quanti-
   tative relationship between scour length and one or
   more of the above mentioned factors.

6. Depth of scour hole:

   - decreases when the particle size of the bed material
     increases ;
   - decreases when the solid apron length is increased.
     The effect of apron lengthening is the greater the
     shorter is the apron to be lengthened.
   - decreases with the provision of end sills. Different
     end sills have different degrees of influence. The
     best shape of end sill for individual cases should
     be selected by investigation.

- decreases with the provision of baffle piers. Different shapes of baffle piers and their arrangement on the solid apron determines the degree of influence on the scour depth.
- increases with the provision of chute blocks ;
- increases along with the increase of discharge intensity ;
- increases with the increase of the Froude number of stream before the hydraulic jump .

It is very difficult to give a firm conclusion on the relationship between tailwater depth and depth of scour although there is a partial agreement between the researchers on the decrease of scour depth when the tailwater depth increases. Additional research data is required to state the relationship with higher certainity.

7. It is not possible to obtain a general quantitative relationship between the scour dimensions and the factors influencing them since there are so many variables involved and the phenomenon of local scour is very complex. In the studies made so far, no two investigators have produced the same quantitative formulation to estimate local scour dimensions. Thus, there are as many empirical relationships as there are investigators of local scour problem in an erodible bed below solid aprons.

8. Prediction of scour depth using eqs. 4.17b and 4.18b should be simple because a straight line graph is obtained in each case when the points of h_{max}/h_o versus t/t_1 from equation 4.17b are plotted on a log-log paper and also when the points of D versus log $(t-t_o)$ from equation 4.18b are plotted on a normal paper. Thus, such straight lines can be plotted using data collected

from short duration of scour observation. The resulting straight line is easily extrapolated to predict the scour depths for longer duration. Knowing the scour depth, one can compute the scour length from the relationship existing between the similar scour hole profiles.

9. Local scour can be partially prevented by dissipating part of the energy of the stream by creating a hydraulic jump in a properly designed basin. The basin depth and width must be proportioned such that the hydraulic jump is neither drownd nor swept out of the basin floor. For a well designed stilling basin the tailwater depth is nearly equal to the conjugate depth after the jump.

10. The appurtenances of stilling basins serve the following purposes:

    End sills:

    - push up the hydraulic jump towards the foot of the spillway;
    - prevent scouring of the erodible bed immediately after the end of the solid apron;
    - improve the velocity distribution across the flow;
    - dentated end sills break the continuity and compactness of the incident nape.

    Baffle piers:

    - dissipate energy mostly by impact action;
    - two rows of staggered blocks improve the velocity distribution.

    Chute blocks:

    - furrow the incoming jet and lift a portion of it from the floor and produce a shorter length of jump;
    - have marginal contribution of energy dissipation.

Different shapes and arrangements of stilling basin
appurtenance have different degrees of contribution for
the prevention of local scour. The suitable shape and
arrangement for individual cases should be determined
by model tests.

11. Bulk air concentration of 15 - 20 % reduces scour by
    5 - 10 % in simple stilling basins. The effect is less
    the more complex is the basin. Despite the latter, it
    appears advisable to consider air entraining possibilities
    without external assistance during the design of
    spillways.

12. In local scour protection of an erodible bed, the
    length to be protected is estimated by scale model
    analysis or by computing using empirical relations.
    The commonly used method of protection is by covering
    the erodible bed with stones of various sizes which
    fulfil the following conditions:

    - Stones that make up the upper layer should withstand
      the action of drag forces to a sufficient degree.
    - The base material should not be capable of passing
      through the voids left between the components of
      the upper layers.

    The first condition is fulfiled by using results from
    model tests and the second by applying the Terzaghi-
    Vicksburg criterion.

13. To establish the bed topography of a scour region, a
    network of measuring points (grid) should be planned
    in advance. Distances are measured by steel rope in
    laboratory flumes and small streams, and by theodolite
    in large rivers. Depths are measured by staff gages
    or by sounding (weighted line) from a boat or
    cableway.

14. Water levels are measured by staff gages installed on rigid structures. Level recorders are used to measure water level changes with time. However, since level recorders are very expensive devices, staff gages must be prefered unless there is a very great need for observation of continuous water level changes with the change of time.

15. The most commonly used instrument to measure flow velocities is the current meter. With this instrument it is possible to measure the velocity at separate points in the flow or to investigate velocities in the whole section (isovels) and also to obtain the mean cross-sectional velocity. Pitot tube is used also to measure velocity at a point in the flow.

16. The discharge in rivers and canals is most frequently estimated from the expression

$$Q = AV \qquad\qquad (7.2)$$

Discharge can also be obtained by measuring stage at a cross-section and by using an already established rating curve for the cross-section. Broad crested notches or weirs based on laboratory studies are used to estimate discharge. On smaller rivers and canals a sharp-edged notch or a Venturi or Parshal measuring flume is used for measuring discharge. Other methods such as dilution gaging are also used for discharge measurement in rivers and canals.

17. Direct measurement of bed load transport is carried out by using grated opening in small streams and by the aid of portable bed load meters in large rivers. Indirect bed load measuring methods include acoustic, electric and optical methods, radioactive and fluorecent

tracers, etc. Suspended sediment concentration is
measured either directly by taking individual or pumped
samples from the flow or indirectly with the aid of
turbidity meters based on the principle of photoelectric
effect.
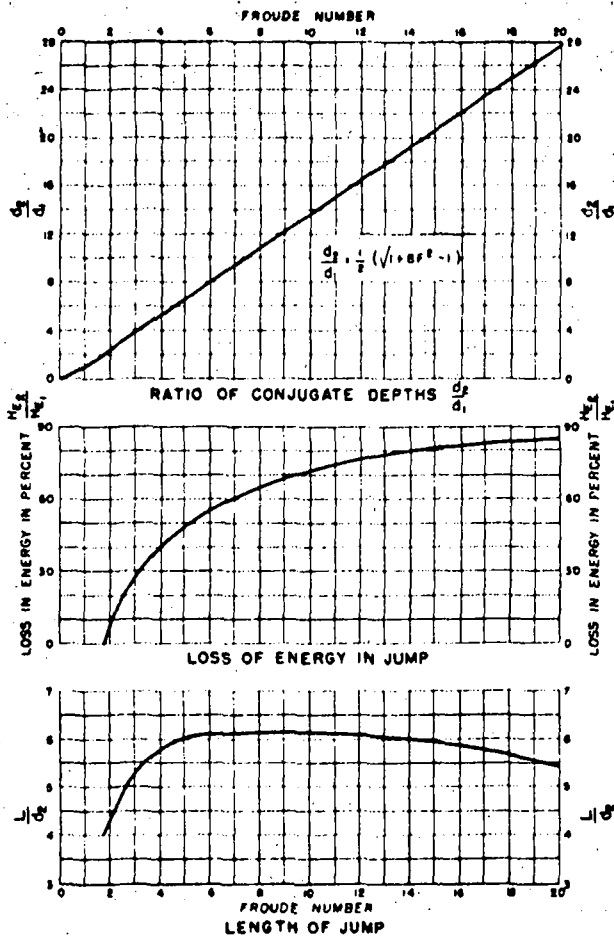
Figure A1. Hydraulic jump properties
in relation to Froude
number./46/
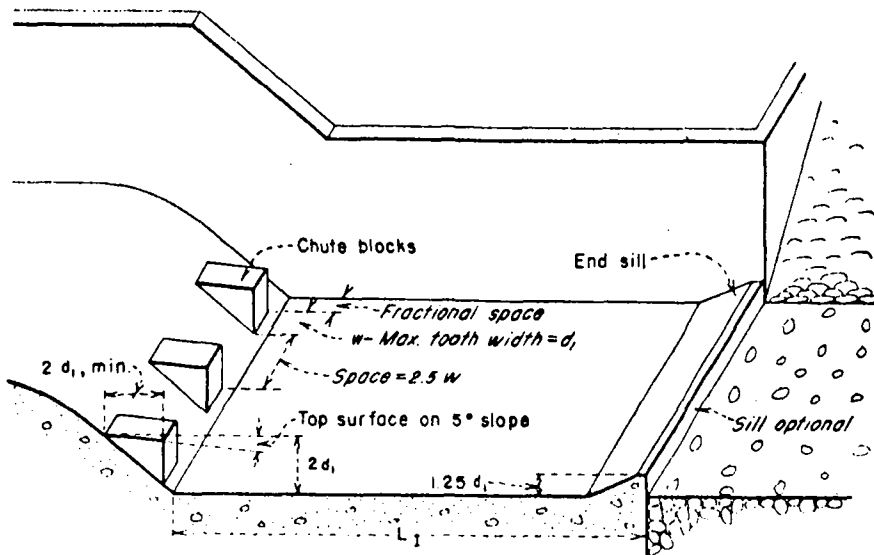
(A) TYPE 1 BASIN DIMENSIONS

FROUDE NUMBER

Chute blocks

End sill

Fractional space

w- Max. tooth width = d_1

Space = 2.5 w

Top surface on 5° slope

Sill optional

2 d_1, min.

2 d_1

1.25 d_1

L_1

(B) MINIMUM TAILWATER DEPTHS

$\frac{T.W. DEPTH}{d_1}$

$\frac{T.W.}{d_2} = 1.1$

$\frac{d_2}{d_1} = \frac{1}{2}\left(\sqrt{1+8F^2}-1\right)$

(C) LENGTH OF JUMP

$\frac{L_1}{d_2}$
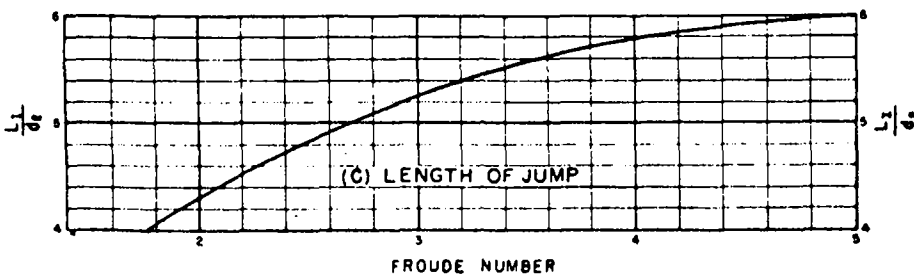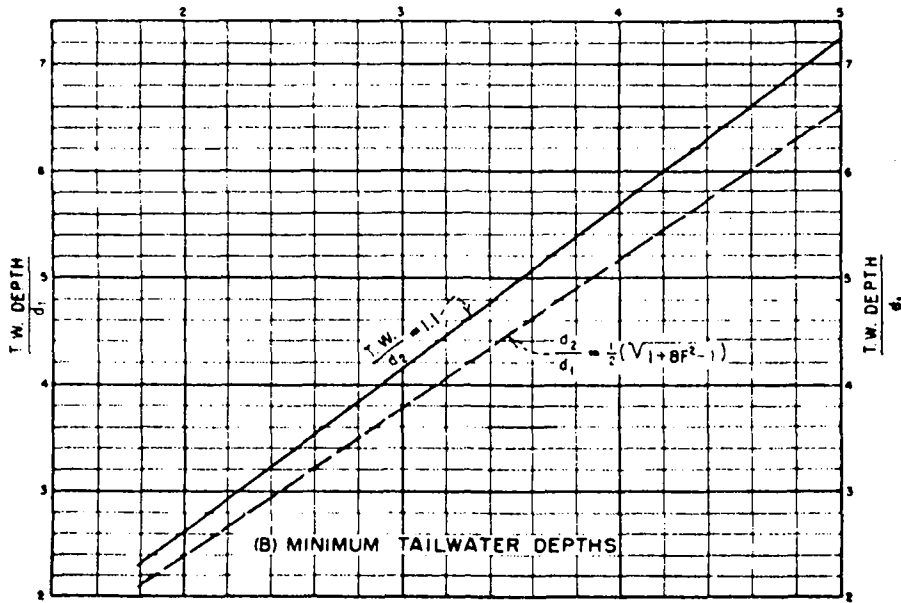
FROUDE NUMBER

Figure A2. Stilling basin characteristics for Froude numbers between 2.5 and 4.5. /46/

(A) TYPE II BASIN DIMENSIONS

(B) MINIMUM TAILWATER DEPTHS

(C) HEIGHT OF BAFFLE BLOCKS AND END SILL

(D) LENGTH OF JUMP
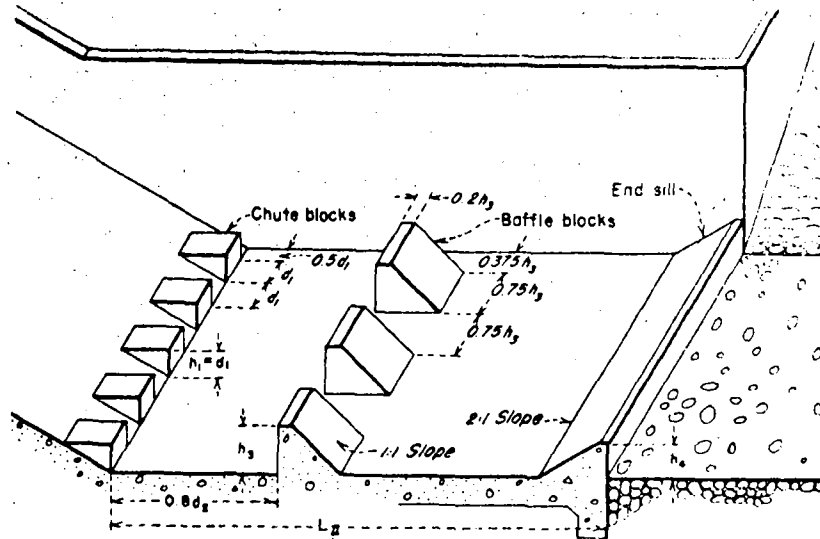
Figure A3.   Stilling basin characteristics for
            Froude numbers above 4.5 where incoming
            velocity does not exceed 50 feet per
            second./46/

(A) TYPE III BASIN DIMENSIONS

(B) MINIMUM TAILWATER DEPTHS
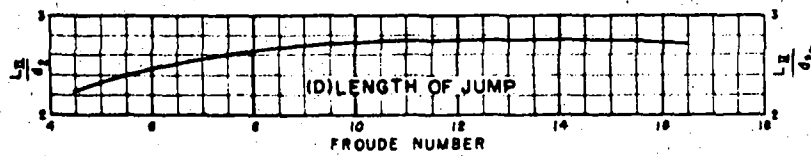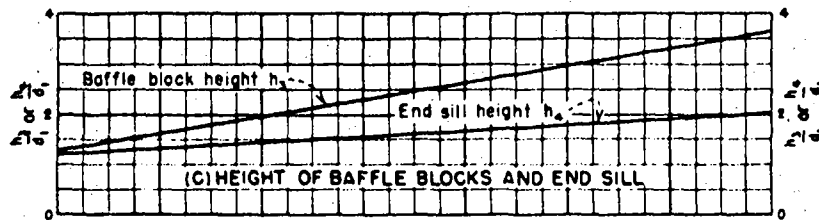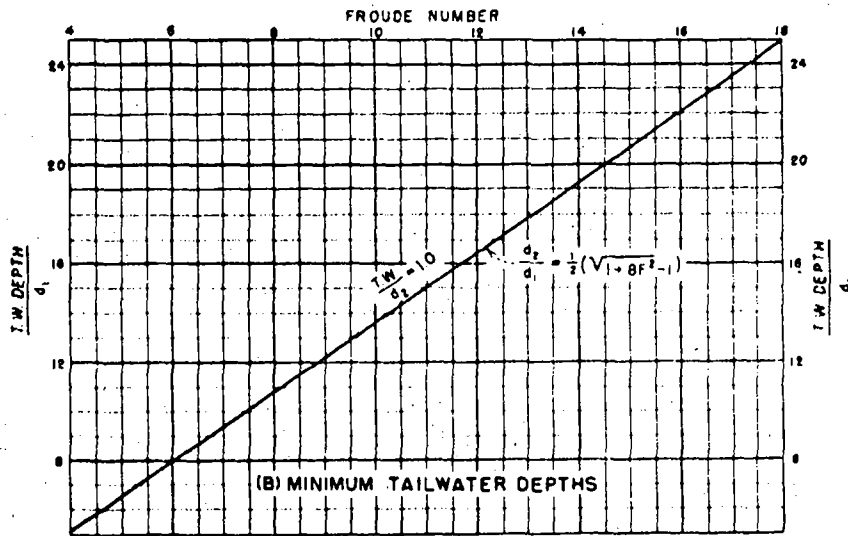
(C) LENGTH OF JUMP

$$\frac{d_2}{d_1} = \frac{1}{2}\left(\sqrt{1+8F^2}-1\right)$$
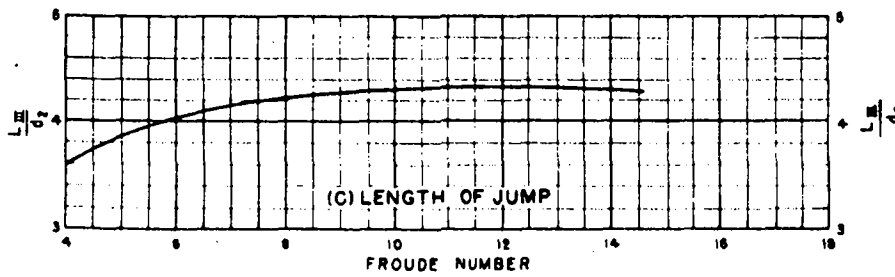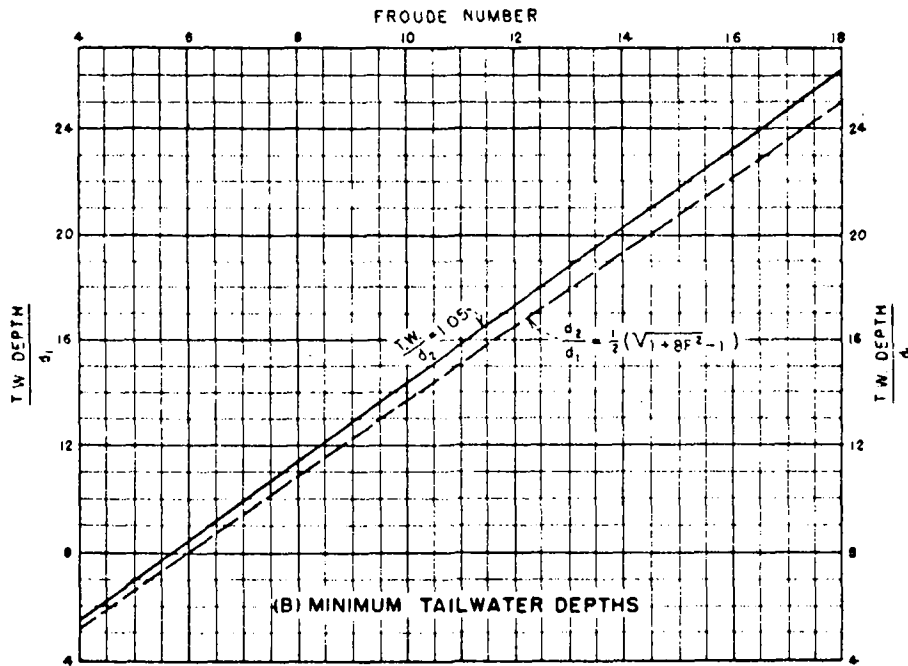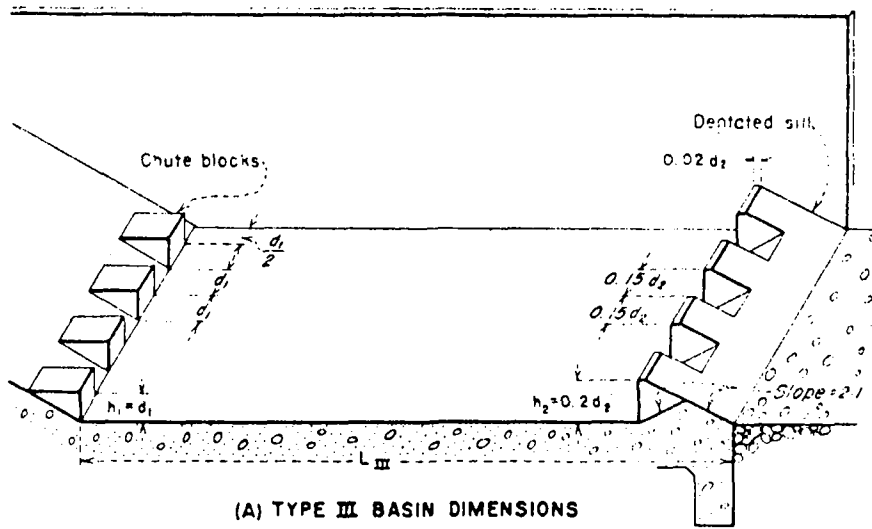
Figure   A4.   Stilling basin characteristics for
Froude numbers above 4.5./46/

REFERENCES

1.   Ahmad, M.,
        Causes of Retrogression Below Islam Barrage and
        Remedial Measures to Cause Accretion and Push the
        Hydraulic Jump to the Toe of the Glacis,
        International Association for Hydraulic Research,
        Report on the Fourth Meeting, Bombay, India, 2-5 .I.
        1951

2.   Ahmad, M.,
        Mechanism of Errosion Below Hydraulic Works,
        Proceedings, Minnesota International Hydraulics
        Convention, Minneapolis, Minnesota
        August, 1953

3.   Altinbilek, H.D.,
        Similarity Laws for Local Scour with Special Emphasis
        on Vertical Circular Pile in Ossillatory Flow,
        Fourteenth Congress of the International Association
        for Hydraulic Research 29 August - 3 September 1971

4.   Altinbilek, H.D., Basmaci, Y.,
        Localized Scour at the Downstream of Outlet Structures
        Commission Internationale Des Grands Barrages,
        Onzieme Congrés des Grands Barrages, Madrid 1973

5.   Blaisdell, F.W., Asce, F., Anderson, C.L., and
        Hebaus, G.G.,
        Ultimate Dimensions of Local Scour,
        Journal of the Hydraulics Division, vol. 107, No. 3
        March 1981

6.   Blench, T., Ahmad, M., Ahmad, N.,
        Scour in Alluvium Below Falls,
        International Association for Hydraulic Structures
        Research,
        Stockholm 7-9 VI 1948

7.   Breusers, H.N.C.,
        Conformity and time Scale in Two-Dimensional Local
        Scour,
        Delft Hydraulics Laboratory, Publication No. 40,
        March, 1965

8.   Breusers, H.N.C.,
      Time Scale of Two Dimensional Local Scour,
      Proceedings, Twelfth Congress of the International
      Association for Hydraulic Research, Volume No. 3,
      Colorado State University, Fort Collins, Colorado,
      USA, 11-14 September 1967

9.   Gatakli, O., Ozal, K., Tandozan, A.R.,
      A Study of Scour at the End of Stilling Basin and
      Use of Horizontal Beams as Energy Dissipators,
      Commission Internationale Des Grands Barrages,
      Onziéme Congrés des Grands Barrages,
      Madrid 1973

10.   Chow, V.T.,
      Open-Channel Hydraulics
      McGraw-Hill Book Company, Inc.,
      New York   Toronto   London,
      Kogakusha Company, LTD., Tokyo
      1959, pp: 393 - 438

11.   De Marchi, G.,
      Experiments on Bed Scouring Downstream Weirs,
      International Association for Hydraulic Structures
      Research, Second Meeting,
      Stockholm 7-9 VI 1948

12.   Einstein, H.A.,
      The Bed Load Function for Sediment Transportation
      in Open Channel Flows,
      U.S. Department of Agriculture, Soil Conservation
      Service, Technical Bulletin No. 1026,
      Washington, D.C., 1950

13.   Fanti, K., Zbikowski, A.,
      Local Scour Downstream From Weirs,
      Commission Internationale Des Grands Barrages,
      Onziéme Congrés des Grands Barrages,
      Madrid 1973

14.   Farhoudi, J., and Smith, K.V.H.,
      Time Scale for Scour Downstream of Hydraulic Jump,
      Journal of the Hydraulics Division, vol. 108, No. 10
      October 1982

15.   Framji, K.K.,
      Scour Below Weirs,
      International Association for Hydraulic Structures
      Research, Second Meeting,
      Stockholm 7-9 VI 1948

16.   Guinea, P.M., Lucas, P., Aspuru, J.J.,
      Selection of Spillways and Energy Dissipators,
      Commission Internationale des Grands Barrages,
      Onziéme Congrés des Grands Barrages,
      Madrid 1973

17.   Gunko, F.G.,
      Macroturbulence of Flows Below Spillways of Medium
      Head Dams and Their Protection Against Undermining,
      Proceedings, Twelfth Congress of the International
      Association for Hydraulic Research, vol. No. 2,
      Colorado State University, Fort Collins, Colorado,
      USA, 11-14 September 1967

18.   Gupta, O.P., Gupta, S.N., Saxena, P.N.,
      Effects of Flood Hydrographs on the Regime of Alluvial
      and Boulder Stage Rivers Above and Below Control
      Structures,
      Proceedings, Twelfth Congress of the International
      Association for Hydraulic Research,
      September 11-14, 1967

19.   Hamid, M.A., Farrant, R.F.T., Ahmad, M.,
      Air Entraining Devices and Their Use in Correcting
      Flow Conditions at Weirs and Canals Falls,
      Proceedings, Minnesota International Hydraulics
      Convention, Minneapolis, Minnesota
      September 1-4 1953

20.   Hartung, F., Csallner, K.,
      The Scouring Energy of the Macroturbulent Flow
      Down-Stream of a Hydraulic Jump,
      Proceedings, Twelfth Congress of the International
      Association for Hydraulic Research, volume No. 3
      Colorado State University, Fort Collins, Colorado
      USA, 11-14 September 1967

21. Hay, N., and White, P.R.S.,
    Effects of Air Entrainment on the Performance of
    Stilling Basins,
    Proceedings, XVIth Congress of the International
    Association for Hydraulic Research, vol. 2,
    Sao Paulo-Brasil, 1975

22. Hellström, B.,
    Measures to Reduce Scour Below Dams,
    International Association for Hydraulic Structures
    Research, Second Meeting,
    Stockholm 7-9 VI 1948

23. Hickox, G.H.,
    Prevention of Erosion below TVA Dams,
    International Association for Hydraulic Structure
    Research, Second Meeting,
    Stockholm 7-9 VI 1948

24. Joglekar, D.V., and Wadekar, G.T.,
    The Effects of Weirs and Dams on the Regime of Rivers
    International Association for Hydraulic Research
    Fourth Meeting, Bombay,
    India 1951

25. Lacey's Stable Channels in Alluvium,
    Paper No. 4736, Inst. of Civil Engineers,
    London, 1930

26. Laursen, E.M.,
    Observations on the Nature of Scour,
    Iowa Institute of Hydraulic Research,
    Iowa City, Iowa, 1952

27. Linsley, Jr. R.K., Kohler, M.A., Paulhus, J.L.H.,
    Hydrology for Engineers,
    McGraw-Hill Book Company, Inc.,
    New York   Toronto   London,
    1958, pp. 52 - 89

28. Lipay, I.E., Pustovoit, V.F.,
    On the Vanishing of Intensive Macroturbulence in Open
    Channel Below Hydraulic Outlet Structure,
    Proceedings, The International Association for
    Hydraulic Research, vol. 2,
    Colorado State University, Fort Collins, Colorado,
    USA, September 11-14 1967

29. Mehrotra, S.C.,
Scale Effects in Model Tests of Rock-Protected
Structures,
Proceedings, vol. 2, XVIth Congress of the International
Association for Hydraulic Research,
Sao Paulo, Brasil, 1975

30. Minor, H.E.,
Local Scours Following A Solid Weir,
Proceedings, vol. 2, XVIth Congress of the International
Association for Hydraulic Research,
Sao Paulo, Brasil, 1975

31. Novak, P., and Cabelka, J.,
Models in Hydraulic Engineering,
Pitman Advanced Publishing Program
Boston London Melbourne,
1981

32. Rajaratnam, N.,
Erosion by Plane Turbulent Jets,
Journal of Hydraulic Research 19, No. 4
1981

33. Rajaratnam, N., Macdougall, R.K.,
Erosion by Plane Wall Jets With Minimum Tailwater,
Journal of Hydraulic Engineering, vol. 109, No. 1,
July 1 1983

34. Rand, W.,
Sill-Controlled Flow Transitions and Extent of
Erosion,
Journal of the Hydraulic Division,
Proceedings of the American Society of Civil Engineers,
No. 4, April 1970

35. Raudkivi, A.J.,
Loose Boundary Hydraulics,
Pergamon Press,
Oxford New York Toronto Paris Sydney
Frankfurt, 1976, pp. 23 - 45

36.   Rebhock, T.,
      Discussion of Paper by Burno & White, Jour.
      Instt. C.E., October 1939, p. 260:
      also discussion of Paper by Butcher & Aitkinson,
      proc. Inst. C.E., vol 235 (1934), p. 256

37.   Ribeiro, A.A., Lemos, F.O., Ramos, C.M.,
      Bed Protection Downstream of A Big Dam Founded in
      Alluvia,
      Commission Internationale Des Grands Barrages,
      Madrid 1973

38.   Ribeiro, A.A.,
      The Macroturbulence Downstream a Stilling Pool.
      Erosion (Scouring),
      Proceedings, vol. 5,
      XVIth Congress of the International Association
      for Hydraulic Research,
      Sao Paulo, Brasil, 1975

39.   Riguelme, L.A., Rivas, I.B.,
      On the Applicability of Systematic Scale Selection
      Methods for Modeling Movable Bed Open Channel Flows,
      International Conference on Water Resources Development,
      Taipei, Taiwan, Republic of China,
      May 12-14, 1980

40.   Schoklitsch, A.
      Prevention of Scour and Energy Dissipation, translated
      by E.F. Wilsey,
      Bureau of Reclamation, Denver, 1937
      (Schoklitsch, A. "Kolkabwehr und Stauraumberlandung"
      Berlin: Julius Springer, pp. 17-183, 1935)

41.   Schoppmann, B.,
      The Mechanics of Flow and Transport of a Progressive
      Scour,
      Proceedings, vol. 2
      XVIth Congress of the International Association
      for Hydraulic Research,
      Sao Paulo, Brasil, 1975

42.   Simons, B.D., and Sentürk, F.,
      Water Resources Publications,
      Fort Collins, Colorado 80522, USA
      1977, pp. 394-496

43. Suryavanshi, B.D., Vaidya, M.P., Choudhury, B.,
     Use of Chute Blocks in Stilling Basin - an Assessment,
     Commission Internationale Des Grands Barrages,
     Madrid 1973

44. Tsuchiya, Y.,
     On the Mechanism of the Local Scour from Flows
     Downstream of An Outlet,
     Proceedings, Twelfth Congress of the International
     Association for Hydraulic Research, vol. No. 3
     Colorado State University, Fort Collins, Colorado,
     USA, 11-14 September 1967

45. Tung, Y.K., Mays, L.W.,
     Optimal Design of Stilling Basins for Overflow
     Spillways,
     Journal of the Hydraulics Division,
     Proceedings of the American Society of Civil Engineers,
     vol 108, No HY 10,
     October, 1982

46. United States Department of the Interior,
     Bureau of Reclamation,
     Design of Small Dams,
     United States Government Painting Office,
     Washington, 1960, pp. 291 - 307

47. Valentin, F.,
     Considerations Concerning Scour in the Case of Flow
     Under Gates,
     Proceedings, Twelfth Congress of the International
     Association for Hydraulic Research, vol. No. 3,
     Colorado State University, Fort Collins, Colorado,
     USA, 11-14 September 1967

48. Meulen, V.D.,
     Three-Dimensional Local Scour in Non-Cohesive
     Sediments,
     Proceedings, vol. 2,
     XVIth Congress of the International Association
     for Hydraulic Research,
     Sao Paulo, Brasil, 1975

49. Vinjé, J.J.,
     On the Flow-Characteristics of Vortices in Three-
     Dimensional Local Scour,
     Proceedings, Twelfth Congress of the International
     Association for Hydraulic Research,
     Colorado State University, Fort Collins, Colorado,
     USA, 11-14 September 1967

50. Watkins, R.D., Aust, M.I.,
    Local Scour in Beds of Sand and Gravel Downstream
    from a Solid Apron,
    Civil Engineering Transactions,
    April 1969

51. Walshaw, A.C., and Jobson, D.A.,
    Mechanics of Fluids,
    Longman Group Limited, London,
    1972, pp. 301 - 302

52. Wu, C.M.,
    Scour At Downstream End of Dams in Taiwan,
    International Association for Hydraulic Research,
    International Symposium on River Mechanics,
    Bangkok, Thailand, 9-12 January 1973

53. Zimmermann, F., and Maniak, U.,
    Scours Behind Stilling Basins with Endsills of
    Baffle Piers,
    Proceedings, Twelfth Congress of the International
    Association for Hydraulic Research, vol. No. 3,
    Colorado State University, Fort Collins, Colorado,
    USA, 11-14 1967